



## Review

## Recent progress on composite desiccants for adsorption-based dehumidification



Yu Zhang, Weining Wang, Xu Zheng\*, Jinliang Cai

*School of Civil Engineering and Architecture, Zhejiang Sci-Tech University, No. 928 Second Road, Xia Sha District, Hangzhou, 310018, Zhejiang, China*

## ARTICLE INFO

**Keywords:**  
 Desiccant coated heat exchanger  
 Fixed bed  
 Rotary wheel  
 Adsorption  
 Desorption

## ABSTRACT

Humidity plays a significant role in both daily life and industrial manufacturing. Adsorption-based dehumidification attracts considerable attention due to advantages of temperature and humidity independent control and great energy-saving potential. For adsorption-based dehumidification systems, desiccants are the basis for optimizing heat transfer and moisture adsorption performance. Despite the rapid advancements in materials science, few systematic classifications concerning composite materials are available. The primary objective of this paper is to provide a holistic and explicit roadmap of recent developments in composite desiccants, directing at its application in adsorption-based dehumidification for energy efficient utilization. Improvements in heat transfer can be achieved by adding high thermal conductivity materials or by reasonably designing structures of dehumidification components. Moisture adsorption is enhanced by combining different desiccants to maximize their functions. Three main categories are classified, that is, salt-embedded composites, porous matrix-polymer composites and polymer-polymer composites. This paper can help to identify the research gaps and explore promising approaches for future study to further enhance the energy efficiency of adsorption-based dehumidification technologies.

## 1. Introduction

With rising living standards, energy consumption and environmental damage are major issues confronting the world today. In response to global climate change and higher outdoor temperatures, households spend an average of 35%–42 % more on electricity for air conditioning [1]. Meanwhile, buildings consume a third of the total global energy and 55 % of building energy consumption comes from heating, ventilation and air conditioning (HVAC) systems [2,3]. Humidity plays a significant role in daily life as well as industrial manufacturing. In particular, the latent heat load for dehumidification accounts for 40 % of the total load [4,5]. Therefore, it is imperative to find an efficient way to deal with the latent heat load.

The most commonly used vapor compression cooling systems are based on the principle of condensation dehumidification. Since the heat and moisture are highly coupled in such systems, the evaporation temperature is below the dew point of process air for dehumidification, and hence the coefficient of performance (COP) is limited. Worse still, reheating is needed sometimes, resulting in additional energy consumption [4,6]. To overcome these weaknesses, an alternative choice is

adsorption-based dehumidification, in which fixed beds and desiccant wheels are successfully commercialized [7]. Compared to fixed beds, rotary wheels exhibit higher dehumidification efficiency for the reason that dehumidification and regeneration can be simultaneously performed. However, both fixed beds and rotary wheels suffer from an intrinsic defect, that is, the outlet air temperature undergoes an upward trend because of the adsorption heat effect and the heat transferred from the regeneration section with the rotation of the wheel [8].

In recent years, a new type of compact dehumidification component named desiccant coated heat exchanger (DCHE) that can achieve isothermal dehumidification and improve the adsorption capacity has attracted widespread attention [9–12]. Isothermal dehumidification is achievable by coating the heat exchanger surface with desiccant materials and introducing an internal cooling/heat source [13–16]. The cooling source is introduced to remove the negative effects of the adsorption heat released by the desiccant, and thereby deal with the sensible heat in the treated air for cooling. Up to now, cold water [9,10,17], hydrofluorocarbons (HFCs) [18–20] and cooling air [21] are often used as cooling sources in the dehumidification process of DCHE systems. Compared to cooling air, cold water and HFCs are more suitable as cooling sources within the system due to their high specific heat

\* Corresponding author.

E-mail address: [cindy1989v@zstu.edu.cn](mailto:cindy1989v@zstu.edu.cn) (X. Zheng).

<b>Nomenclature</b>	
<b>Symbols</b>	
$D$	Diffusivity, $\text{m}^2 \cdot \text{s}^{-1}$
$k$	kinetic constant, $\text{s}^{-1}$
$m$	Fitting parameter for the modified LDF model
$p$	Vapor pressure
$P_0$	Saturated vapor pressure at adsorption temperature
$q$	Water uptake, $\text{g} \cdot \text{g}^{-1}$
$r$	Radius, m
$t$	Time, s
$x$	Thickness coordinate, m
$\delta$	Thickness, m
<b>Subscripts</b>	
$ad$	Adsorption
$d$	Desiccant
$de$	Desorption
$eq$	Equilibrium
$init$	Initial
$intra$	Intraparticle
$p$	Particle
<b>Abbreviations</b>	
AC	Activated carbon
ARI	American Air-Conditioning and Refrigeration Institute
ASHRAE	American Society of Heating, Refrigerating and Air-Conditioning Engineers
$\text{CaCl}_2$	Calcium chloride
$\text{CH}_3\text{COONa}$	Sodium acetate
$COP$	Coefficient of performance
$COP_{th}$	Thermal coefficient of performance
$D_{avg}$	Average moisture removal capacity
DCHE	Desiccant coated heat exchanger
DFHE	Desiccant coated fin-and-tube heat exchanger
DMHE	Desiccant coated microchannel heat exchanger
EG	Expanded graphite
ENG-TSA	Expanded natural graphite treated with sulfuric acid
FCNT	Functionalized multiwalled carbon nanotube
FHE	Fin-and-tube heat exchanger
HFCs	Hydrofluorocarbons
HVAC	Heating, ventilation and air conditioning
IUPAC	International Union of Pure and Applied Chemistry
KCOOH	Potassium formate
LDF	Linear driving force
$\text{LiCl}$	Lithium chloride
MHE	Microchannel heat exchanger
MOF	Metal-organic framework
$Nu$	Nusselt number
PAA	Polyacrylic acid
PAAS	Sodium polyacrylate
PNIPAM	Poly(N-isopropylacrylamide)
PVA	Polyvinyl alcohol
$Re$	Reynolds number
SA	Sodium alginate
SASG	Alginate-silica gel
SEM	Scanning electronic microscope
SG	Silica gel

capacity. In addition, heat for the regeneration process can be obtained from low-grade heat sources such as solar energy [22] and waste heat [23].

In the past decades, extensive research has been conducted towards adsorption-based dehumidification including three different scales, namely, the desiccant scale [24–26], the device scale [27–29] and the system scale [30–32]. For adsorption-based dehumidification systems, desiccants are responsible for the removal of water vapor from processed air and are related to heat transfer and moisture adsorption performance. The dehumidification performance is still constrained by the poor sensible heat handling ability and low thermal conductivity of desiccant materials. Besides, single desiccant materials such as porous physical adsorbents, chemical salts and hygroscopic polymers have defects of low moisture adsorption capacity or high regeneration temperatures or potential corrosion and several publications have given a comprehensive overview of single materials [13,15]. Besides, there are several review articles regarding desiccants in adsorption-based dehumidification systems [3,6,12,14,15]. However, to the authors' knowledge, there is a rare comprehensive literature review of publications regarding the comprehensive classification of composite desiccants. Thus, the primary emphasis of this review lies on composite desiccant materials utilized in dehumidification components, involving two dimensions, enhancement in heat transfer and improvement in moisture adsorption.

Principles of adsorption-based dehumidification including fixed bed dehumidification, rotary dehumidification and DCHE-based dehumidification are briefly introduced. Then, how to improve the heat transfer and moisture adsorption performance of desiccants is classified and summarized. The enhancement of heat transfer is mainly considered with the incorporation of high thermal conductive materials and the structure of dehumidification components. The improvement of moisture adsorption takes into account from the perspective of combinations

of several single desiccants, including salt-embedded composites, porous matrix-polymer composites and polymer-polymer composites. Furthermore, the comparative study including the equilibrium adsorption quantity and desorption ability, the adsorption-desorption kinetics curves of different composite desiccants and thermal COP of DCHE-based systems are involved and discussed. Finally, conclusions and perspectives for future study are outlined.

## 2. Principles of adsorption-based dehumidification

### 2.1. Dehumidification components

Adsorption-based dehumidification components can be divided into three types: a fixed bed [33]; a rotary wheel [30] and a DCHE [34]. A fixed bed is filled with dehumidifying materials to dehumidify the air (Fig. 1a). During the dehumidification process, humid air flows through the bed device to obtain dry air. During the regeneration process, hot dry air was supplied to take away adsorbed moisture in desiccants. From Fig. 1b, desiccant materials are impregnated into a support structure of a wheel. The wheel is divided into dehumidification and regeneration sections by clapboard. When it constantly rotates, in dehumidification section, the process air is dried by the desiccant. Meanwhile, the regeneration air is humidified after being heated by a heater and desorbing the water from the wheel. The greatest advantage of the rotary desiccant dehumidification is that dehumidification and regeneration can be carried out at the same time, while fixed beds are superior for noise- and rotor-free operation. However, both fixed bed desiccant dehumidifiers and rotary desiccant wheels suffer from an intrinsic defect because of the adsorption heat effect.

The operating principles of a DCHE are illustrated in Fig. 1c. The desiccant material is coated on the surface of the DCHE and isothermal adsorption/desorption is achievable by introducing the internal

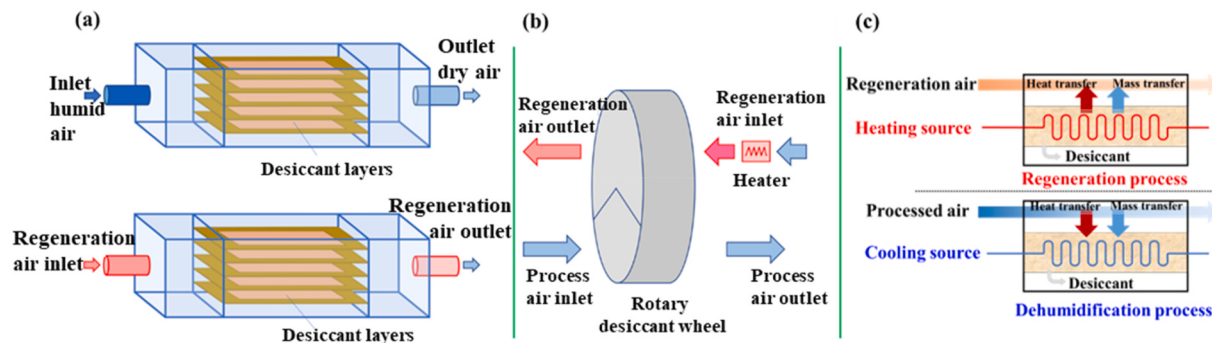


**Fig. 1.** Principle of operation of dehumidification components: (a) a fixed bed [33], (b) a rotary wheel [30], (c) a DCHE [34] (taking the most commonly used fin and tube heat exchangers as an example).

cooling/heat medium. For the regeneration process, the heating source is connected to the DCHE. The hot and dry regeneration air undergoes heat and mass transfer with the coated desiccants and adsorbed water in the desiccant is subsequently discharged into the air. For the dehumidification process, the cooling source is connected to the DCHE. The moist processed air flows over the surface of the DCHE and moisture is adsorbed by the desiccant. The two modes shift back and forth so that desiccants can be repeatedly used.

## 2.2. Performance indexes to evaluate desiccants

The desiccant is responsible for the removal of water vapor from processed air and is the basis for optimizing the heat transfer and moisture adsorption performance of the adsorption-based dehumidification. There are five possible interactions between solids and water vapor [35]: physical adsorption of water vapor on the surface of solids, hydration of solids with water vapor to form crystal hydrate, capillary condensation in micropores, deliquescence, and absorption of concentrated solutions into dilute solutions, as shown in Fig. 2. Physical adsorption and capillary condensation occur mainly in porous desiccants, while the mechanism of salt is primarily hydration reaction, liquid dissociation and absorption. Polymers rely on their internal structure with a rich cross-linking network in contact with water to generate capillary phenomena that promote the rapid diffusion of moisture [36].

Absorption isotherm and dynamic adsorption capacity are two important indicators to evaluate promising desiccant for adsorption-based dehumidification. Desiccants used in adsorption-based dehumidification should possess large adsorption capacity and can be easily regenerated. Adsorption isotherms are available for assessing the adsorption and desorption capabilities of desiccants. It characterizes the affinity for water vapor at different relative pressures ( $P/P_0$ ) [37]. Fig. 3a shows the classification of six main water adsorption isotherms according to the International Union of Pure and Applied Chemistry (IUPAC) [38–40]. Type I stands for super hydrophilic materials where the moisture increases dramatically at low relative pressures. Adsorption isotherms with types II, IV, and VI can also be considered as hydrophilic materials because they possess a large amount of

hygroscopicity at low and middle relative pressures. Type III is taken to be representative of hydrophobic or low hydrophilic materials, which have a sharp increase in water adsorption capacity when the relative pressure is close to 1. Type V corresponds to materials with low water adsorption capacity at low relative pressures and a clear S-shaped curve at middle and high relative pressures.

In general, desiccants corresponding to type I, II, IV or VI isotherms exhibit large water adsorption capacity at low relative pressures but more difficult to regenerate, while desiccants with type III and V isotherms usually have low water uptakes at low relative pressures but easier to regenerate. Fig. 3b illustrates an ideal working cycle of desiccants used in adsorption-based dehumidification. Since environments with higher humidity needs dehumidification, desiccants that can adsorb more water (that is, larger  $W_{ad}$ ) in higher humidity ratio under the same air temperature (i.e. higher  $P/P_0$ ) are more promising. Besides, in desorption process, desiccants with less adsorption capacity (that is, lower  $W_{de}$ ) at lower humidity ratio can be more easily regenerated.  $\Delta W_{cycle} = W_{ad} - W_{de}$  then denotes the theoretical cyclic dehumidification capacity of an adsorption-based dehumidification system.

As another important indicator, adsorption/desorption kinetics can influence the cycle time of adsorption-based dehumidification. Adsorption/desorption rates ( $k_{ad}/k_{de}$ ) of desiccants are calculated by empirical kinetic models [42–45], as shown in Fig. 4. Fick's diffusion (FD) model is applicable for describing intraparticle diffusion via spherical particles as well as bulk diffusion via plane layers, which is more precise over 50 % of the equilibrium adsorption quantity [45]. Linear driving force (LDF) model expresses the vapor diffusion behavior on the surface of desiccants, assuming that the desiccant adsorbs in a monolayer form at the adsorption sites [44]. Modified LDF model takes into account the internal diffusion behavior of the desiccant, in the form of monolayer-multilayer adsorption [42]. Besides, polymer swelling model is suitable for hygroscopic gel [42]. For adsorption-based dehumidification, most scholars adopt LDF model due to its simplicity and reasonable accuracy in fitting water vapor adsorption/desorption kinetics.

In addition to indexes of high adsorption capacity, good regeneration ability and fast adsorption/desorption kinetics, desiccants should also

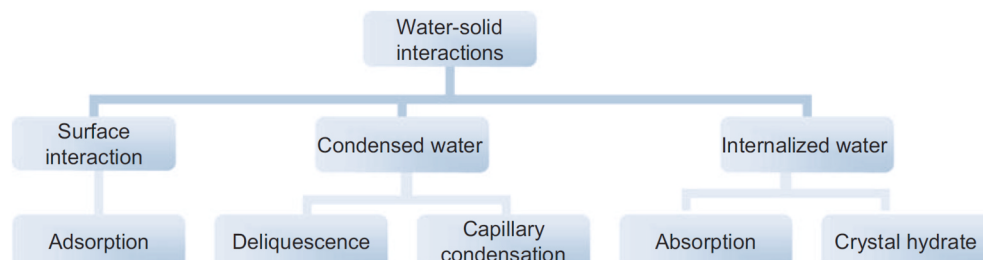


**Fig. 2.** Interactions between solids and water vapor [35].

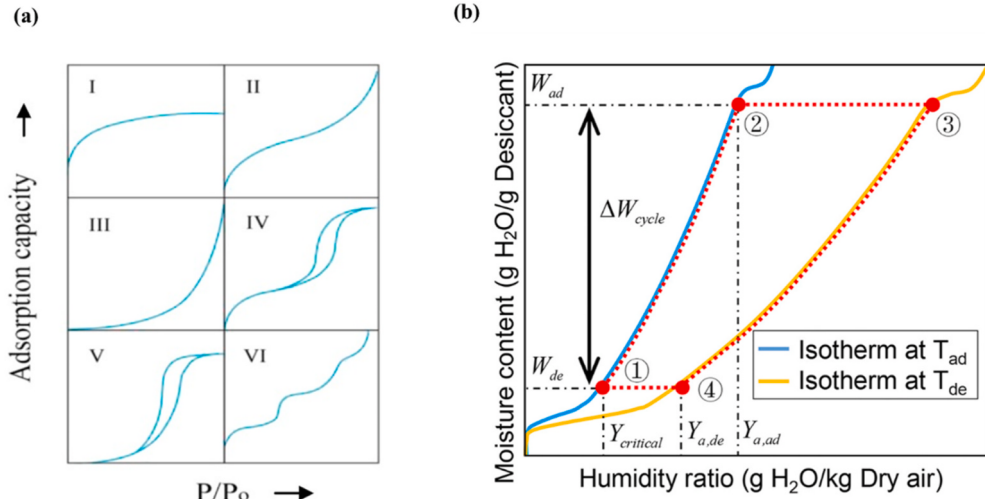


**Fig. 3.** Adsorption isotherms for desiccants used in adsorption-based dehumidification: (a) Classification of water adsorption isotherms according to IUPAC [38]; (b) An ideal cycle for adsorption and desorption [34,41].

Models	Fick's diffusion (FD)	Linear driving force (LDF)	Modified LDF
Equation	$\frac{\partial q_d}{\partial t} = D \frac{\partial^2 q_d}{\partial x^2}$	$\frac{\partial q_d}{\partial t} = k_{LDF} (q_{d,eq} - q_d)$	$\frac{\partial q_d}{\partial t} = \frac{15m}{t} \left( \frac{D_{intra} t}{r_p^2} \right)^m (q_{d,eq} - q_d)$
Linearsed form	spherical particle: $\ln \left( 1 - \frac{q_d - q_{d,init}}{q_{d,eq} - q_{d,init}} \right) = -\frac{\pi^2 D}{r^2} t + \ln \left( \frac{6}{\pi^2} \right)$ plane layer: $\ln \left( 1 - \frac{q_d - q_{d,init}}{q_{d,eq} - q_{d,init}} \right) = -\frac{\pi^2 D}{4\delta^2} t + \ln \left( \frac{8}{\pi^2} \right)$	$\ln(q_{d,eq} - q_d)$ $= -k_{LDF} t + \ln(q_{d,eq} - q_{d,init})$	$\ln(q_{d,eq} - q_d)$ $= -k_{LDF,m} t^m + \ln(q_{d,eq} - q_{d,init})$
References	[42,43,45]	[46,61,62,66,68,73,75,80,87,89,103]	[42]

**Fig. 4.** Empirical kinetic models for adsorption/desorption.

have other features such as long-term stability, nontoxicity, proper cost and etc.

### 2.3. Applications

The above mentioned dehumidification components can be applied in a variety of fields, including dehumidification, humidification, heat pumps and atmospheric water harvesting [17,20,46,47]. Fig. 5a shows schematic diagram of solar assisted dehumidification system. When the temperature of the ambient air entering the tube rises, relatively hot air is carried away to the dehumidifier by a fan. The hot air is used to eliminate the moisture on the wheel surface and ensure the continuity of the dehumidification process. The regeneration air is moistened by sweeping away the moisture accumulated in the dryer wheel and is discharged from the dehumidifier. Owing to the continuous dehumidification of the dryer wheel with regeneration air, the process air entering the dehumidifier is constantly dehumidified [44].

The schematic diagram of the DCHE-based heat pump with HFCs such as R410A and R32 introduced is shown in Fig. 5b. The system consists of two DCHEs, a compressor, an expansion valve and a four-way directional valve for continuous dehumidification. Two DCHEs always have one acting as a condenser and the other as an evaporator through the conversion of a four-way directional valve, providing a constant supply of cold and low humidity air to the room. The refrigerant in the pipeline provides the required cooling capacity for the desiccant and the waste heat from condensation is available for the regeneration of the DCHE.

The working principle diagram of the atmospheric water harvesting systems using sorption bed is presented in Fig. 5c, which is divided into water vapor adsorption during the night and condensation water

harvesting during the day. Outdoor air enters the adsorption bed by a fan and water vapor in the air is adsorbed by desiccants. The inlet valve is closed at the end of adsorption and an electric heater was employed to imitate the solar collector heating process. After the adsorption bed is heated, the high-temperature and high-humidity gas flows through the condenser and condenses into liquid water, which drips into the collection tank at the bottom.

This paper mainly focuses on composite desiccant materials used in adsorption-based dehumidification. In the subsequent sections, composite desiccants are divided into two dimensions: heat transfer and moisture adsorption, as shown in Fig. 6a and(b). Improvements in heat transfer can be achieved by adding high thermal conductivity materials or by reasonably designing structures of dehumidification components. Moisture adsorption is enhanced by combining different single materials to maximize their strengths, which is classified into three main categories: salt-embedded composites, porous matrix-polymer composites and polymer-polymer composites.

### 3. Enhancement of heat transfer

Researchers have reported that the introduction of additives such as nano silver powder [48], expanded graphite (EG) [49], graphite sulfide [50,51], nano-copper [52] and carbon nanotube [53,54] is able to improve thermal conductivity of coated desiccants. Thermal conductivities and scanning electronic microscope (SEM) pictures of composites modified with different high thermal conductivity additives are displayed in Fig. 7a-(d). The findings on the influence of high thermal conductivity additives on desiccants are summarized in Table 1. The positive effect on the thermal conductivity such as reduction of desiccant particle gap and provision of an oriented heat transfer structure can

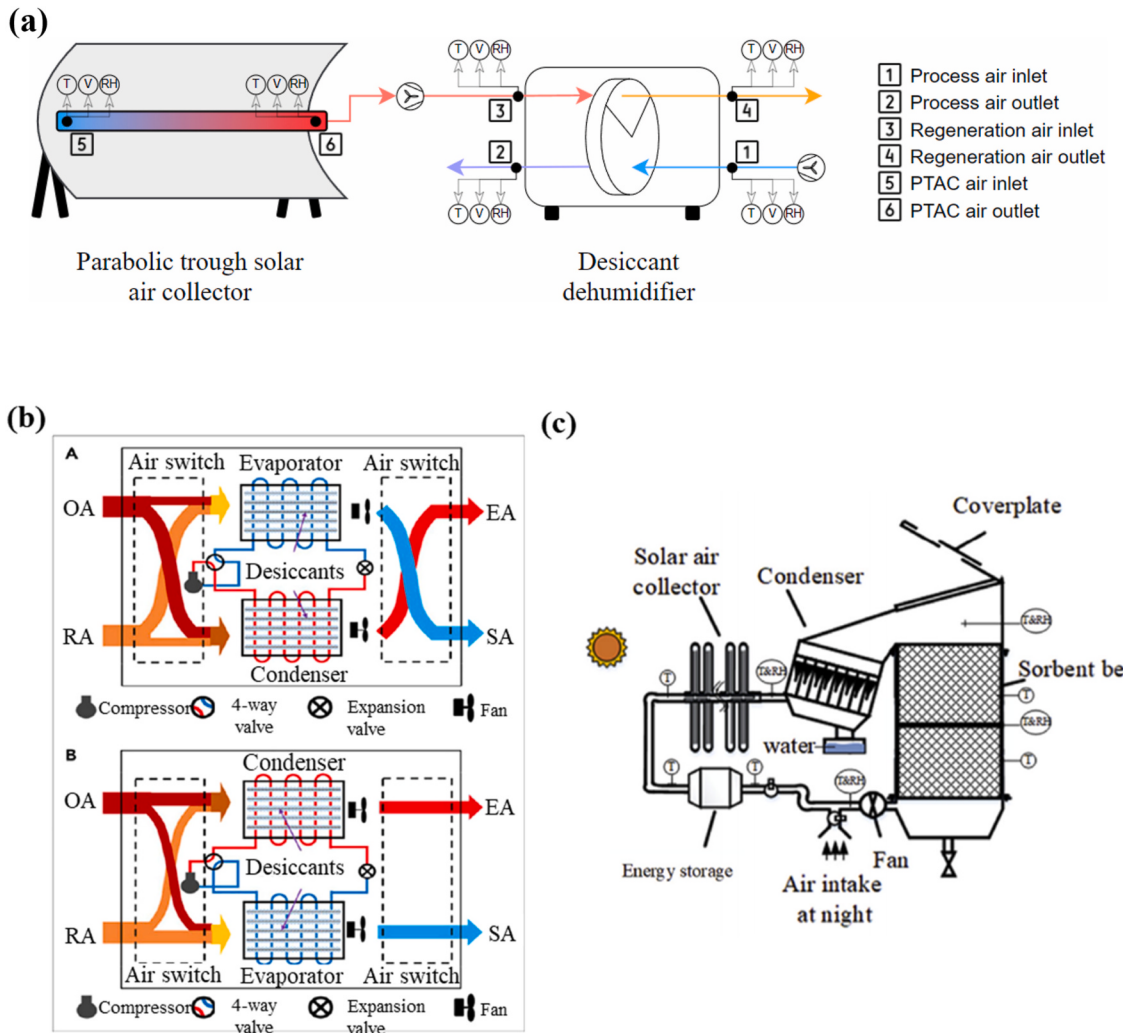


**Fig. 5.** Working principles of rotary desiccant dehumidification (a) [44], DCHE-based heat pump (b) [20] and fixed bed-based atmospheric water harvesting (c) [47].

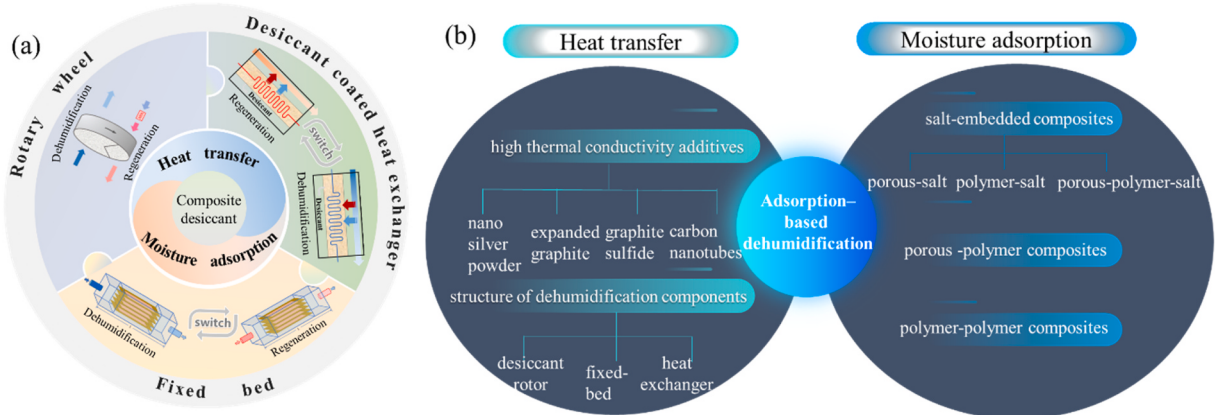


**Fig. 6.** General overview of the entire text (a) and heat transfer and moisture adsorption enhancement for adsorption-based dehumidification (b).

be observed in the SEM images. For example, an experimental study by Zheng et al. [51] showed that the thermal conductivity of composite silica gel reached a maximum of  $19.1 \text{ W m}^{-1} \text{ K}^{-1}$  with an increase in the proportion of expanded natural graphite treated with sulfuric acid (ENG-TSA) at the bulk density of  $225 \text{ kg m}^{-3}$ , which was 270 times higher than  $0.07 \text{ W m}^{-1} \text{ K}^{-1}$  of pure silica gel.

These composite desiccants have moisture adsorption capacity. By

adding nano-silver powder, the dynamic adsorption performance of composite FAPO-34 samples was improved and their adsorption rate coefficients increased by 6–103 % compared with a non-additive sample [48]. Besides, the regeneration temperature of a composite FAPO-34 coated heat exchanger can be  $10^\circ\text{C}$  lower than a pure FAPO-34 coated heat exchanger. Similarly, a consolidated composite silica gel that added ENG-TSA at a bulk density of  $200 \text{ kg m}^{-3}$  possessed the best

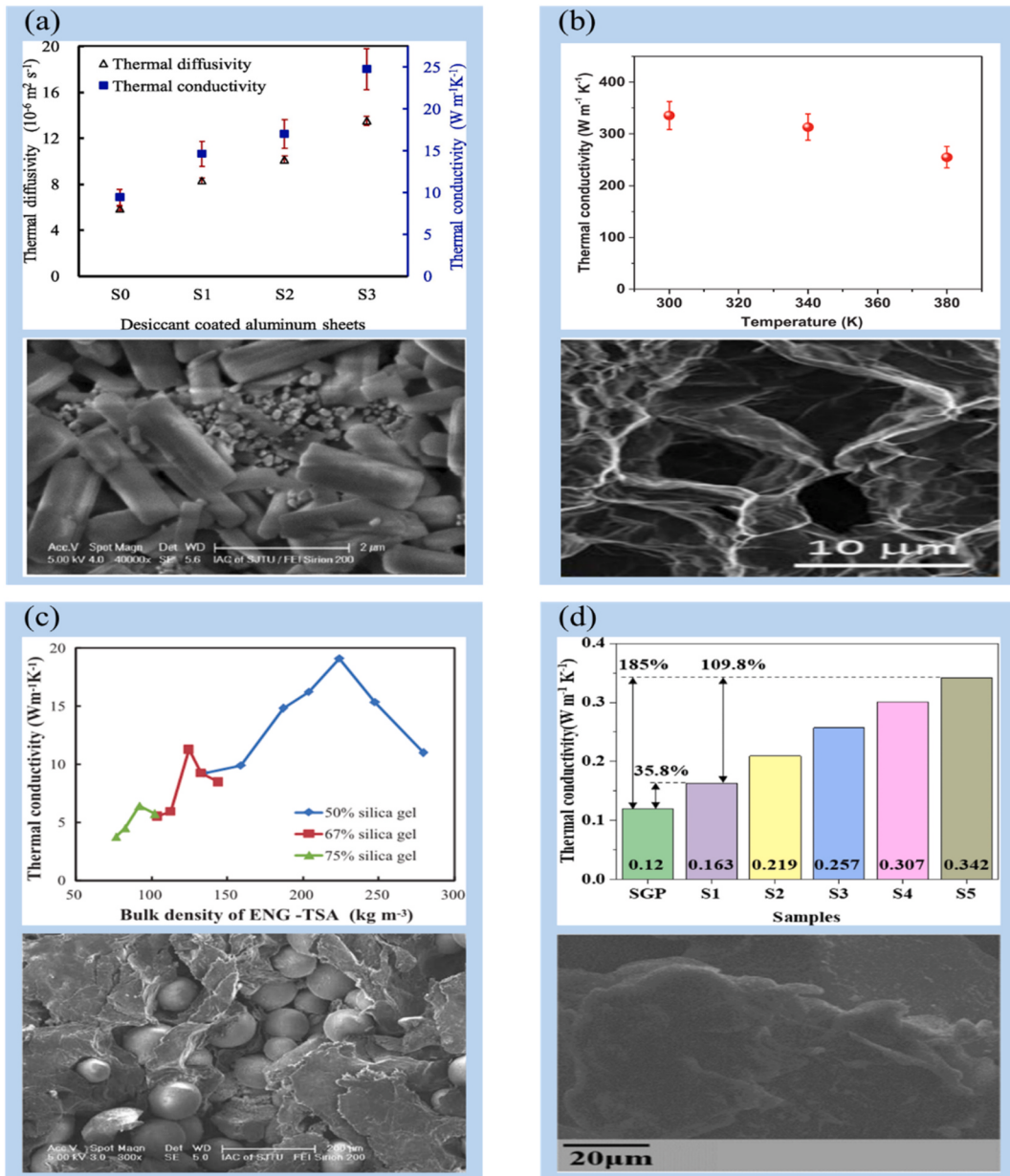


**Fig. 7.** Properties of composites modified with different high thermal conductivity additives: (a) nano silver powder [48]; (b) expanded graphite [49]; (c) ENG-TSA [51]; (d) nano-copper [52].

dynamic water adsorption capacity and water adsorption rate coefficient, which was 2–3 times better than those of loose silica gels [51]. Starkova et al. [54] calculated the equilibrium water contents of epoxy mixed with expanded graphite and multiwall carbon nanotubes using a diffusion-relaxation model, which was 1.06 and 1.16 times greater than that of neat epoxy, respectively.

Specifically, apart from thermal conductivity of materials, heat transfer performance of adsorption-based dehumidification systems can be affected by structures of dehumidification components. For rotary wheels systems, desiccant rotor substrate will affect the dehumidification performance. Substrates using aluminum foil has good heat transfer property but cost too much. Though substrates made of glass fiber paper, ceramic fiber or plastics such as polystyrene have inferior heat transfer performance, they are widely used due to advantages of good dehumidification performance and low cost, as shown in Fig. 8.

For fixed beds systems, packed beds are the most common form (Fig. 9a). However, the main shortcoming is the need for a high-powered

fan because of the large pressure drop caused by the presence of densely packed desiccants. Recently, thin multilayer packed beds (Fig. 9b) have been applied in dehumidification since relatively lower pressure drop can be achieved. In addition, honeycomb sorption bed (Fig. 9c) with unblocked mass transfer channels is proposed, which can significantly optimize the water vapor adsorption-desorption performance.

For a DCHE-based dehumidification system, the types of heat exchangers can affect its heat transfer performance. In addition to the most widely used fin and tube heat exchangers (Fig. 1c), Venegas et al. [15] had summarized other heat exchanger types used in DCHE systems, including microchannel, finless tube, wire and tube, metal foam, graphite plate and lattice, as shown in Fig. 10. However, except for microchannel heat exchangers, there is few comparative studies between other alternatives and the most widely used fin and tube heat exchangers.

Sun et al. [58] developed a desiccant coated fin and tube heat exchanger (DFHE) and a desiccant coated microchannel heat exchanger

**Table 1**

The findings on the influence of high thermal conductivity additives on desiccants.

Desiccants	Thermal conductivity ( $\text{W}\cdot\text{m}^{-1}\cdot\text{K}^{-1}$ )	Notes	Ref
Nano-silver powder/FAPO-34	10.7–24.8	The excellent conductivity of nano-silver powder as well as the filling of voids in FAPO-34 improves the conduction pathway, making the desorption rate 1.3–2.3 times higher than that of pure FAPO-34.	[48]
Expanded graphite ribbon	254–335	The longitudinal thermal conductivity of expanded graphite ribbon is higher than that of some carbon fibers, which contributes to the rational thermal design of EG-based composites.	[49]
ENG-TSA/SG	9.8–19.1	The thermal conductivity of composites is closely related to the bulk density of ENG-TSA and the percentage of silica gel. With the increase in bulk density of ENG-TSA, the thermal conductivity increases and then decreases.	[51]
Nano-copper/SG/polyvinyl pyrrolidone	0.22–0.34	The thermal conductivity of composite desiccant with the NC content of 1.6 wt% is improved by 185 % over the parent silica gel powder, with an effective enhancement of thermal conductivity and excellent adsorption/desorption stability.	[52]
Carbon nanotube/SG/CaCl <sub>2</sub>	0.664	The water vapor adsorption capacity of the composite is 5 times higher than that of single SG and its adsorption capacity and thermal conductivity are highly sustainable with no significant decrease during cycling.	[53]
Carbon nanotube/epoxy	0.29	Nanocomposites have a higher water adsorption capacity compared to pure epoxy resins due to the ability of nanoparticles to modify the molecular arrangement of the polymer chain segments during the curing process and facilitate the generation of voids and extra open polar groups in the epoxy.	[54]

(DMHE) using silica gels (Fig. 11a). Dynamic performance, heat transfer coefficient and moisture removal capacity were studied, as shown in Fig. 11b–d. Compared to the DFHE, the DMHE exhibits mass transfer performance but superior heat transfer coefficient. For example, the

maximum instantaneous moisture removal capacity of the DMHE is 32 % lower than that of the DFHE (Fig. 11b), while the heat transfer coefficients of DMHE are 2.0–2.9 times higher than the DFHE (Fig. 11c). Since the mass transfer area of the DFHE being three times that of the DMHE, the average removal moisture of the DFHE is greater when air velocity is less than  $1.5 \text{ m s}^{-1}$  (Fig. 11d). Whereas, the moisture removal per unit area of the DMHE is always around 150 % better than that of the DFHE. In general, the heat and mass transfer performance of DMHE is advantageous over DFHE at the same mass transfer area.

#### 4. Improvement of moisture adsorption

Desiccant as a medium for moisture adsorption between a dehumidification component and the water vapor in the air to be treated. The moisture adsorption performance and water vapor adsorption capacity of desiccants are closely related. The hygroscopic properties of a single desiccant material are weak, one or two desiccants need to be added to it for additional moisture adsorption capacity. As an important parameter to measure the performance of the desiccant, the equilibrium adsorption capacity reflects its ultimate hygroscopic ability under different relative pressures ( $P/P_0$ ).

##### 4.1. Salt-embedded composites

###### 4.1.1. Porous matrix-based composites

The physical porous desiccant materials such as silica gel (SG) [59, 60], activated carbon (AC) [61, 62], zeolite [63–65] are widely used in adsorption-based dehumidification systems due to their cheap price and high porosity. They mainly realize adsorption through the water vapor pressure difference between the internal pores of desiccant materials and the surrounding air, resulting in a low water vapor adsorption capacity.

Moisture adsorption properties can be effectively enhanced by adding hygroscopic salts such as lithium chloride (LiCl) and calcium chloride (CaCl<sub>2</sub>) to a single porous material [66, 67]. To clarify the relationship between solution concentration and moisture adsorption, an experimental study by Zheng et al. [66] demonstrated the dynamic water adsorption capacity of SG/LiCl enhanced with the increase of the concentration of LiCl (10 wt% to 40 wt%) and the maximum equilibrium adsorption capacity was  $0.3 \text{ g g}^{-1}$  at  $20^\circ\text{C}$ &70 % RH, an enhancement of 200 % over neat silica gel. Later, the AC/SG/LiCl composite desiccant was produced to increase the density of the material for enhancing dehumidification performance [61]. The results showed that the equilibrium adsorption capacity with the addition of LiCl was  $1.14 \text{ g g}^{-1}$  at  $30^\circ\text{C}$ &80 % RH, which was 4.5 times higher than that of pure AC (see Fig. 12). The non-coincidence of adsorption and desorption capacity is caused by the ring hysteresis phenomenon due to capillary coalescence.

The adsorption capacity of composite desiccants with the addition of LiCl is confirmed to increase significantly, but the highly corrosive salt poses a potential hazard to the heat exchanger. To alleviate this deficiency, organic weak acid salts such as potassium formate (KCOOH) and

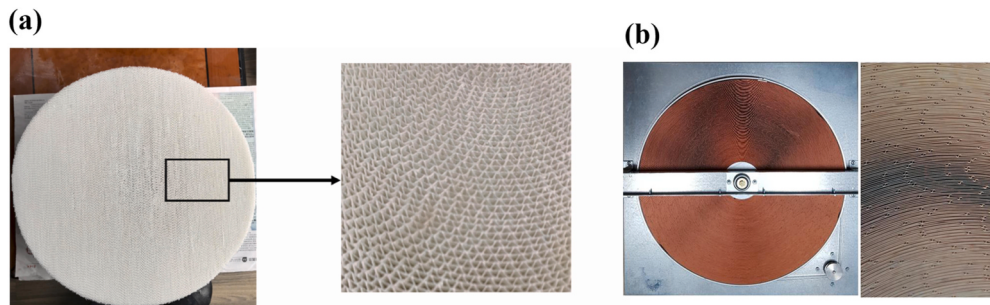


Fig. 8. Images of desiccant rotor substrates: (a) Glass fiber paper [55], (b) polystyrene [56].

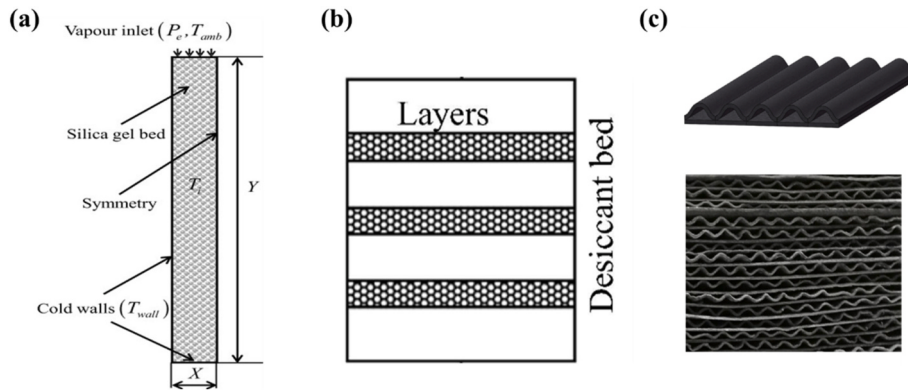


Fig. 9. Types of adsorption beds: (a) packed bed [57], (b) thin multilayer packed beds [6], (c) honeycomb-shaped [32].

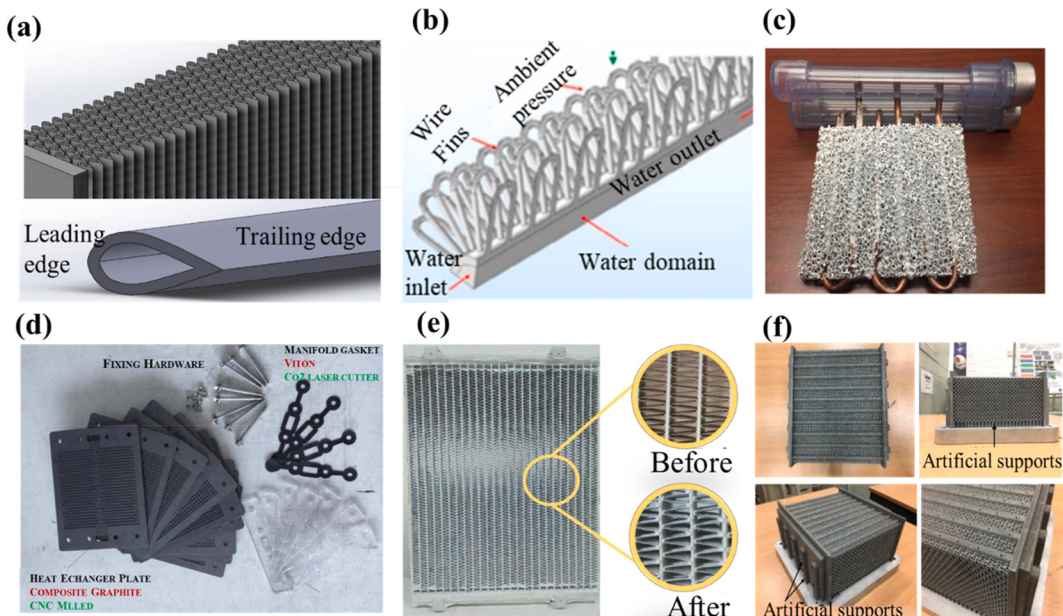


Fig. 10. Other type of heat exchangers: (a) finless tube; (b) wire and tube; (c) metal foam; (d) graphite plate; (e) microchannel; (f) lattice reproduced from Ref. [15].

sodium acetate ( $\text{CH}_3\text{COONa}$ ) are applied to prepare composite desiccant materials [17,68]. Table 2 demonstrates the adsorption capacity and properties of porous matrix-salt composite desiccant materials. Although the organic weak acid salt reduces the corrosiveness of components, it also weakens its adsorption capacity. For example, the water vapor equilibrium adsorption capacity of SG/KCOOH [17] is 15 % lower than that of SG/LiCl [66] at 20 °C & 80 % RH.

In practical applications, the dehumidification/humidification ability is determined not only by the adsorption capacity of unit mass desiccant ( $\text{g H}_2\text{O/g desiccant}$ ), but also by the density and heat capacity of desiccant, desiccant coated amount per unit surface, and so on. In other words, a desiccant with high adsorption capacity of unit mass but low density, the coated mass amount of desiccant is not high. So the moisture removal rate may lower than desiccants with relative low adsorption capacity but high density. For example, a study by Zheng et al. [62] showed that although the dynamic adsorption capacity of ACF/LiCl was superior to that of AC/LiCl, its dehumidification capacity was inferior due to the low density resulting in restriction of coating mass (see Fig. 13).

#### 4.1.2. Polymer-based composites

Polymer desiccant is a kind of macromolecule containing hydrophilic groups and a three-dimensional cross-linked network structure, which

has the advantages of large moisture adsorption capacity and rapid moisture adsorption rate. Hygroscopic polymer desiccants are gradually implemented in dehumidification, atmospheric water harvesting, air conditioning and other fields due to their adsorption capacity being 2–6 times higher than that of ordinary physical porous desiccants [69–71]. Fig. 14 lists the adsorption capacity of single physical porous desiccants and pure polymer desiccants from various researches. A comparative study by Chang et al. [72] demonstrated the adsorption abilities of a sodium polyacrylate coated heat exchanger can be 20%–50 % superior to that of a silica gel coated heat exchanger at high relative humidity conditions (70 % RH–80 % RH).

In recent years, several investigations on the modification of polymers with halogenated salts have been reported. The addition of different concentrations of LiCl to polyvinyl alcohol (PVA) by Vivekh et al. [46] suggested the equilibrium adsorption capacity was proportional to the concentration of LiCl and the maximum effective value was limited to 50 wt% due to the deliquescent phenomenon. The adsorption capacity of PVA/LiCl (50 wt%) composite desiccant was 178 % of its original weight at 80 % RH. Vivekh et al. [73] added KCOOH of 50 wt% to sodium polyacrylate (PAAS) obtaining its equilibrium adsorption capacity of  $0.93 \text{ g g}^{-1}$  at 30 °C & 70 % RH, which was 3.58 times higher than that of the SG/KCOOH (75 wt%) composite desiccant. To avoid leakage of the salt solution, an appropriate mass fraction of LiCl solution

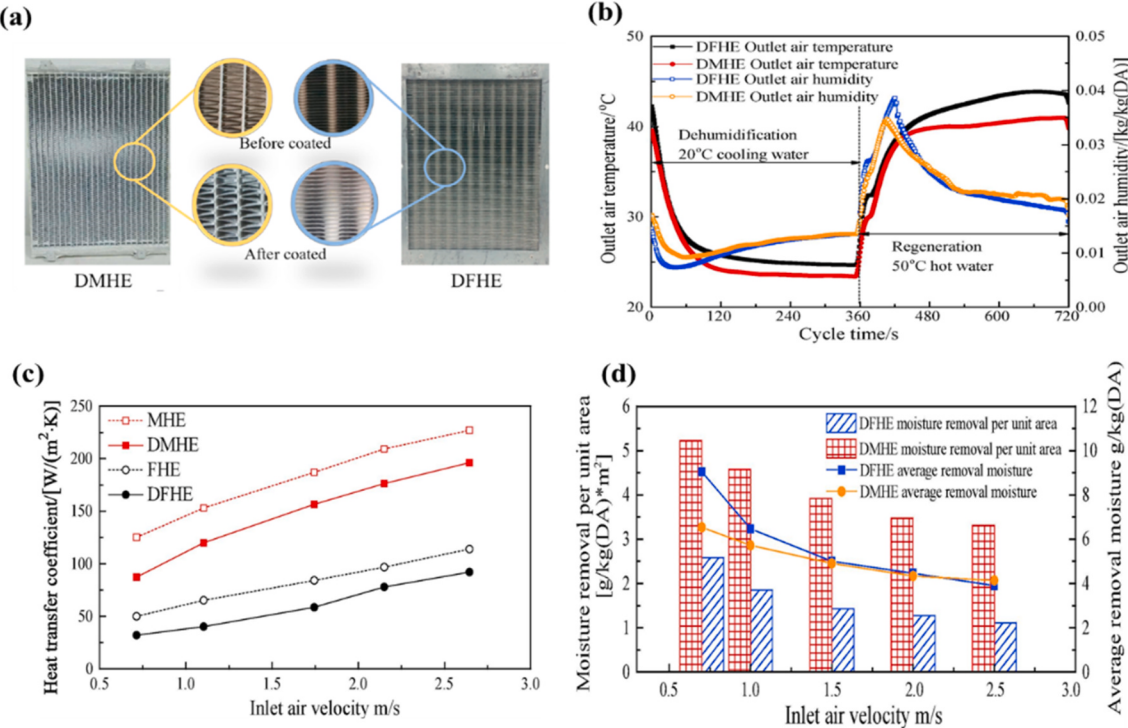


**Fig. 11.** Comparison study between DFHE and DMHE: (a) Photos; (b) dynamic performance of outlet air temperature and humidity at 28 °C&70 % RH; (c) heat transfer coefficient; (d) mass transfer performance [58].

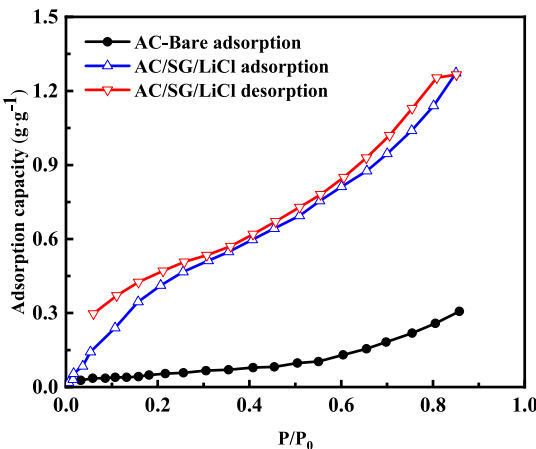


**Fig. 12.** Water adsorption isotherms of AC and AC/SG/LiCl at 30 °C [61].

(18 wt%) was chosen to MIL-100(Fe) by Luo et al. [74] and the resulting composite desiccant showed excellent adsorption capacity compared to single MIL-100(Fe) at high humidity (>60 % RH), as shown in Fig. 15.

The adsorption capacity and properties of certain polymer-salt composite desiccant materials are summarized in Table 3. It can be seen that the adsorption capacity of polymer-salt composite desiccant is related to the type of polymer and the type and concentration of the salt solution impregnated. Polymers are primarily categorized into polymer electrolytes and metal-organic frameworks (MOFs). From Tables 3 and it can be observed that as a MOF material, the adsorption capacity of MIL-100(Fe) after compounding it with LiCl is superior, which is about 8 times higher than that of SG/LiCl [67] composite desiccant under similar operating conditions. The incorporation of MOF in the composite desiccant enhances the adsorption capacity, which is preferable to the porous matrix-salt composite desiccant.

#### 4.1.3. Porous matrix-polymer-based composites

Recently, a combination of porous physical desiccant and hydroscopic polymer has been considered as a matrix with improved adsorption capacity through the addition of the salt solution. The purpose of this process is to enhance the water adsorption capacity of the composite desiccant at medium relative pressure.

A thermo-responsive material consisting of Poly(N-isopropylacrylamide) (PNIPAM), SG and LiCl developed by Ma et al. [80] had an adsorption capacity of 1.7 g g<sup>-1</sup> at 20 °C&70 % RH (Fig. 16) and can be regenerated at a low temperature of 40 °C. A comparison of SG/LiCl and PNIPAM/SG/LiCl reveals the grafted SG has more LiCl compounded in it and the adsorption performance is improved. Zheng et al. [81] obtained alginate-silica gel (SASG) composite desiccant by cross-linking with CaCl<sub>2</sub> and the water adsorption capacity increased sharply at the relative pressure of 0.4–0.5 compared with silica gel, as shown in Fig. 17. Besides, it can be seen that SASG has a water adsorption capacity difference of 0.76 g g<sup>-1</sup> between an adsorption condition (80 % RH) and a regeneration condition (30 % RH), more than twice that of SG. The binary polymeric salt composite obtained by Entezari et al. [82] was composed of sodium alginate (SA) modified with LiCl and CaCl<sub>2</sub> and functionalized multiwalled carbon nanotube (FCNT), which had a water vapor adsorption capacity of 5.6 g g<sup>-1</sup>.

Although the equilibrium water vapor adsorption capacity of the porous matrix-based composites increases with the added hydroscopic salt, the maximum value is difficult to reach 1 g g<sup>-1</sup>. The adoption of porous-polymer-based composites is a promising solution to this problem. The adsorption capacity and properties of porous-polymer-salt composite desiccant materials are summarized in Table 4. The adsorption capacity of porous matrix-polymer-based composites can be observed to be higher than that of porous matrix-based under the similar operating conditions [62,66,80].

#### 4.2. Porous matrix-polymer composites

Hygroscopic salts can cause corrosion to the system components and

**Table 2**

Adsorption capacity and properties of porous matrix-salt composite desiccant materials.

Desiccant	Preparation	Pore volume (cm <sup>3</sup> ·g <sup>-1</sup> )	Average pore size(nm)	Surface area (m <sup>2</sup> ·g <sup>-1</sup> )	Adsorption temp. &P/P <sub>0</sub>	Adsorption capacity (g·g <sup>-1</sup> )	Desorption temp. (°C)	Ref
SG/LiCl	Impregnation with 10 wt % LiCl	0.34	8.9	143	20 °C; 0.7	0.24	100	[66]
SG/LiCl	Impregnation with 20 wt % LiCl	0.30	9.3	135	20 °C; 0.7	0.26	100	[66]
SG/LiCl	Impregnation with 30 wt % LiCl	0.28	9.5	127	20 °C; 0.7	0.28	100	[66]
SG/LiCl	Impregnation with 40 wt % LiCl	0.25	8.4	120	20 °C; 0.8	0.46	100	[66]
SG/LiCl	Impregnation with 30 wt % LiCl	–	–	–	30 °C; 0.9	0.24	–	[67]
SG/KCOOH	Impregnation with 75 wt % KCOOH	0.092	–	47.9	30 °C; 0.7	0.26	90	[68]
SG/KCOOH	Impregnation with 75 wt % KCOOH	–	–	–	20 °C; 0.8	0.39	–	[17]
AC/SG/LiCl	Impregnation with 40 wt % LiCl	0.29	2.5	457	30 °C; 0.8	1.14	90	[61]
AC/LiCl	Impregnation with 45 wt % LiCl	0.32	3.4	384	20 °C; 0.7	0.9	115	[62]
ACF/LiCl	Impregnation with 49 wt % LiCl	0.20	2.0	393	20 °C; 0.7	1.35	90	[62]

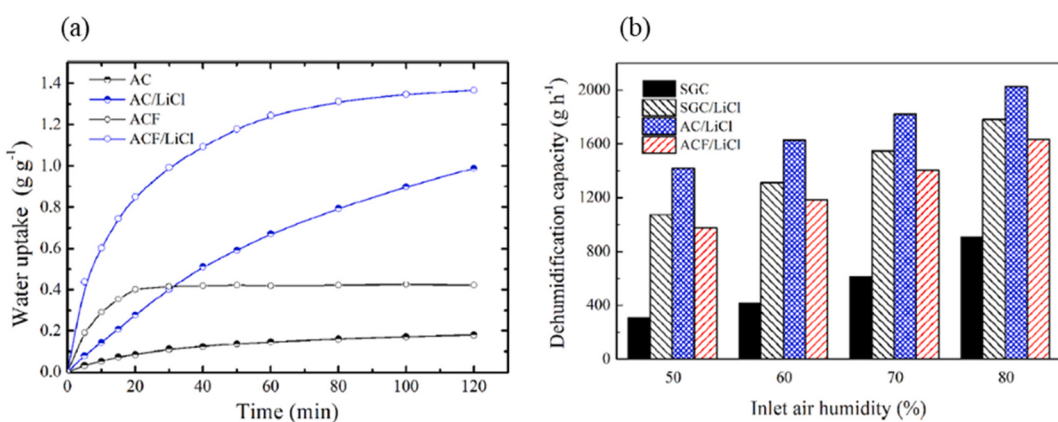


Fig. 13. Water sorption kinetics (a) and dehumidification capacity (b) of different desiccants [62].

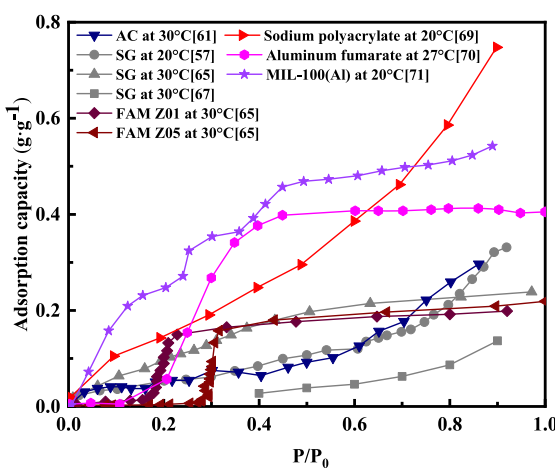


Fig. 14. Adsorption isotherms of single physical porous desiccants and pure polymer desiccants from various researches.

reduce the lifespan of the equipment. Hence, more and more scholars focus on the study of salt-free composite desiccants in view of practical applications.

SG has the advantage of high porosity and stable adsorption, and it is

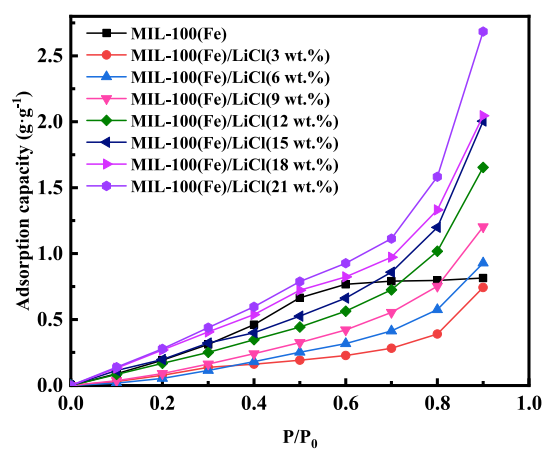


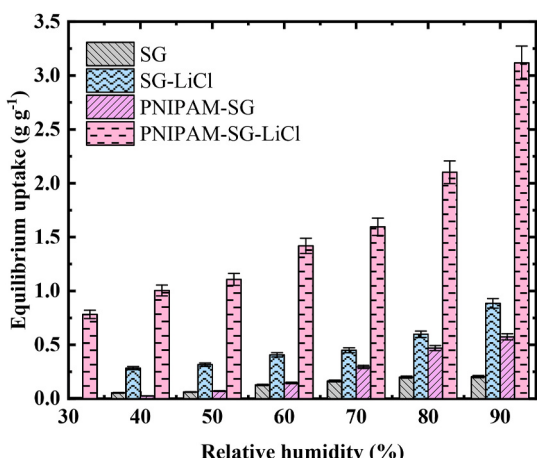
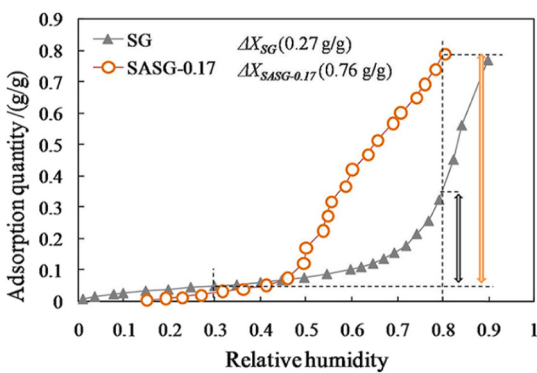
Fig. 15. Adsorption isotherms of LiCl@MIL-100(Fe) with different LiCl mass fraction at 25 °C [74].

often chosen as a matrix. Chen et al. [83] reported that when mixing SG, polyacrylic acid (PAA) and PAAS in the ratio of 10:1:1, the adsorption capacity of composite desiccant was enhanced by 41 % compared to that of pure silica gel at 25 °C&70 % RH. The SG/PAAS/polypropylene fibers composite desiccant produced by Antonellis et al. [84] had an

**Table 3**

Adsorption capacity and properties of polymer-salt composite desiccant materials.

Desiccant	Preparation	Pore volume (cm <sup>3</sup> ·g <sup>-1</sup> )	Average pore size(nm)	Surface area (m <sup>2</sup> ·g <sup>-1</sup> )	Adsorption temp. &P/P <sub>0</sub>	Adsorption capacity (g·g <sup>-1</sup> )	Desorption temp. (°C)	Ref
PVA/LiCl	Mixture of PVA and 50 wt% LiCl with water	–	–	–	30 °C; 0.8	1.34	60–80	[46]
PAAS/KCOOH	Mixture of PAAS and 50 wt% KCOOH with deionized water	–	–	–	30 °C; 0.7	0.93	40–70	[73]
LiCl@MIL-100 (Fe)	Impregnation with 18 wt% LiCl	0.20	0.9	323	25 °C; 0.9	2.05	85	[74]
PAAS/LiCl	Addition of 50 wt% LiCl to 2 wt% PAAS solution	–	–	–	30 °C; 0.8	2.54	60–80	[75]
MIL-101(Cr)/ LiCl	Impregnation with 15 wt% LiCl	0.39	1.20	753	25 °C; 0.8	1.88	–	[76]
MIL-101(Cr)/ CaCl <sub>2</sub>	Impregnation with 25 wt% CaCl <sub>2</sub>	0.14	0.87	236	25 °C; 0.8	1.30	–	[76]
MIL-101(Cr)/ CaCl <sub>2</sub>	Filtration of a 1:6 mass ratio suspension of MIL-101 (Cr) and CaCl <sub>2</sub>	0.99	–	1876	25 °C; 0.9	1.25	–	[77]
Aluminum fumarate/LiCl	Impregnation with PVA:LiCl = 1:1.25	0.19	2.65	286	27 °C; 0.8	1.59	50–80	[78]
PAAS/LiCl	Impregnation with 2.5 mol L <sup>-1</sup> LiCl	–	–	4.68	25 °C; 0.9	2.76	< 80	[79]

**Fig. 16.** Equilibrium water vapor adsorption capacity of different desiccants at 20 °C [80].**Fig. 17.** Adsorption isotherms of water vapor on SASG and SG at 20 °C [81].

adsorption capacity of 0.32 g g<sup>-1</sup> at relative humidity equal to 90 % with reasonable mechanical strength and thermal stability.

In addition, AC and zeolite-like molecular sieves possess a wide variety of framework structures and their specific S-shape characteristic shows potential for application in adsorption-based dehumidification systems [38]. The adsorption isotherms of water vapor on SG, AC and aluminophosphate zeolites are presented in Fig. 18. Qin et al. [85]

obtained a composite desiccant material consisting of SAPO-34 powder and hybrid polymer whose maximum adsorption capacity was unaffected by the binder due to the binder embedding the adsorbent filler. The maximum water vapor adsorption capacity of the composite sample (0.51 g g<sup>-1</sup>) made from preferred coconut shell AC and 50 wt% PAAS solution by Chen et al. [86] was 3.1 times that of pure AC at 20 °C & 90 % RH.

Compared to a single physical desiccant material, the added polymer enhances the moisture adsorption capacity of desiccants. The adsorption capacity and properties of above mentioned and other porous-polymer composites are listed in Table 5. It can be seen that the equilibrium adsorption capacity of the salt-free composite is slightly weakened compared to the salt-embedded composite.

#### 4.3. Polymer-polymer composites

Polymers featuring high water adsorption capacity and low regeneration temperatures are of continuing interest. Polymers are mainly divided into polymer electrolytes and MOF. Polymer electrolytes are high molecular polymers with ionic groups on most of the chain units and possess strong water vapor adsorption capacity. MOFs are crystalline porous materials with topological structures formed by inorganic clusters and organic ligands interconnected in multiple dimensions, exhibiting large surface areas and tunable pore sizes. Therefore, it is possible to replace the conventional physical porous materials described in the above section.

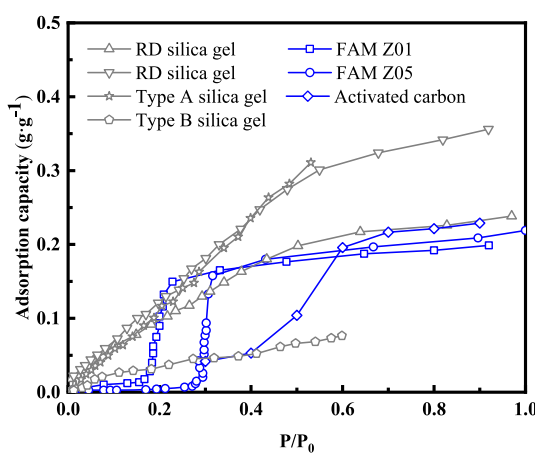
A novel concept “MOF on MOF” is proposed for the in-situ generation of MOF coating layer on metal matrix. This method does not rely on the binder, thus avoiding clogging of pores of porous desiccants. Hermes et al. [90] earlier worked on the formation of [Pd@MOF-5]@SAM membranes of approximately 500 nm thickness on Au. However, the metal substrate in this method is used as a simple carrier for the MOF, and therefore the synthesized MOF lacks sufficient coating density and water vapor adsorption capacity. Afterward, the hybrid MOF layer consisting of MIL-96 and MIL-100 grown on an Al substrate made by Yang et al. [91] could reach 0.48 g g<sup>-1</sup> at 20 °C & 90 % RH, which was close to that of pure MIL-100(Al), as shown in Fig. 19. Although the equilibrium adsorption capacity of hybrid MOF layer is not as high as that of MIL-96(Al) and MIL-110(Al) at low relative humidity, it increases rapidly above 40 % RH. The low cost and easy handling of in situ synthesis of MOF on substrates make large-scale production of MOF possible.

Since polymers possess porous and hygroscopic properties, the adsorption capacity of water vapor can be enhanced through polymer-

**Table 4**

Adsorption capacity and properties of porous-polymer-salt composite desiccant materials.

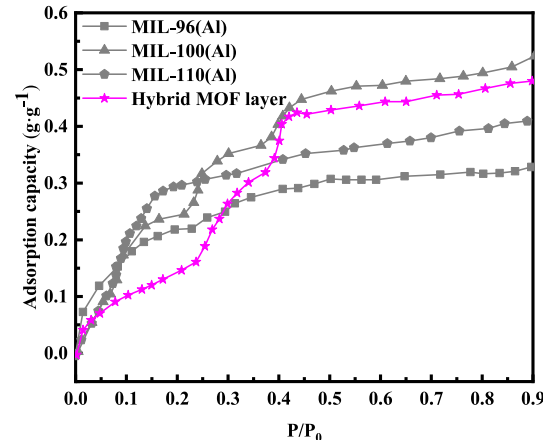
Desiccant	Preparation	Pore volume (cm <sup>3</sup> ·g <sup>-1</sup> )	Average pore size(nm)	Surface area (m <sup>2</sup> ·g <sup>-1</sup> )	Adsorption temp. &P/P <sub>0</sub>	Adsorption capacity (g·g <sup>-1</sup> )	Desorption temp. (°C)	Ref
SG/ PNIPAM/ LiCl	Grafting PNIPAM onto SG, then impregnation with 30 wt% LiCl	0.29	13.2	89.1	20 °C; 0.7	1.7	40–50	[80]
SG/SA /CaCl <sub>2</sub>	Adding SA to SG suspension, then injection into 5 wt% CaCl <sub>2</sub>	0.25	—	17.7	20 °C; 0.8	0.8	< 120	[81]
FCNT/SA /LiCl	Adding SA to 5 wt% FCNT, then injection into LiCl solution	—	—	—	25 °C; 0.7	3.7	—	[82]
FCNT/SA /CaCl <sub>2</sub>	Adding SA to 5 wt% FCNT, then injection into CaCl <sub>2</sub> solution	—	—	—	25 °C; 0.7	2.1	—	[82]
FCNT/SA /LiCl + CaCl <sub>2</sub>	Adding SA to 5 wt% FCNT, then injection into CaCl <sub>2</sub> solution and impregnation with LiCl solution	—	—	—	25 °C; 0.7	5.6	< 80	[82]

**Fig. 18.** Adsorption isotherms of different desiccants: RD silica gel, FAM Z01 and FAM Z05 at 30 °C from Ref. [65,87]; type A and type B silica gel at 30 °C from Ref. [38]; activated carbon at 20 °C from Ref. [86].

polymer composites. The [BOHmim][Zn<sub>2</sub>Cl<sub>5</sub>]@MIL-101 (Cr) with multi-adsorption sites was designed by Gao et al. [92] for overcoming the pore volume limitations of conventional porous desiccant materials and enabling the regeneration at a low temperature of 40 °C. The composite desiccant consisting of MIL-160 (Al) and polymerized 25 % microencapsulated phase change material developed by Qin et al. [93] could be used to alleviate indoor temperature and humidity fluctuations, with a maximum water vapor uptake of 0.36 g g<sup>-1</sup> at 30 °C&80 % RH.

The water vapor adsorption capacity of PNIPAM@MIL-101(Cr) produced by Karmakar et al. [94] was 5.8 and 3.9 times that of pure PNIPAM and MIL-101(Cr) respectively, and 98 % of the water obtained could be released at 40 °C&40 % RH.

Polymer-polymer composites are safe and environmentally friendly, but MOFs are only in the laboratory stage of development and not in mass production due to the high cost. However, the introduction of “MOF on MOF” concept enables the in-situ growth of MOF on metal substrates, which significantly reduces the cost of MOF production and increases application potential in adsorption-based dehumidification

**Fig. 19.** Water adsorption isotherms of several MOFs at 20 °C [91].**Table 5**

Adsorption capacity and properties of porous-polymer composite desiccant materials.

Desiccant	Preparation	Pore volume (cm <sup>3</sup> ·g <sup>-1</sup> )	Average pore size(nm)	Surface area (m <sup>2</sup> ·g <sup>-1</sup> )	Adsorption temp. &P/P <sub>0</sub>	Adsorption capacity (g·g <sup>-1</sup> )	Desorption temp. (°C)	Ref
SG/Aluminum fumarate	Impregnation with 25 wt% aluminum fumarate	0.32	2.55	506.4	27 °C; 0.8	0.70	—	[78]
SG/PNIPAM	Free radical polymerization with PNIPAM and SG in ethanol solution	0.62	13.4	169.1	20 °C; 0.9	0.55	40–50	[80]
SG/PAA/PAAS	Mixture of SG: PAA: PAAS = 10:1:1 with water	0.2	7.0	152.9	25 °C; 0.9	0.51	40–50	[83]
SG/PAAS/polypropylene fibers	Mixture of ingredients with 35.5 % mass fraction of vinyl glue	—	—	—	50 °C; 0.9	0.32	60	[84]
SAPO-34/hybrid polymer	Impregnation with hybrid polymer	—	—	—	30 °C; 0.9	0.27	80–150	[85]
AC/PAAS	Impregnation with 50 wt% PAAS	—	—	—	20 °C; 0.9	0.51	70	[86]
Glass fiber/MIL-100 (Fe)	Dry gel conversion, crystallized at 433K	0.8	2.2	1441	25 °C; 0.9	0.55	80	[88]
MCM-41@EMIM Ac	Impregnated with 95 % pure EMIM Ac	0.001	—	1.441	25 °C; 0.7	0.49	50–80	[89]

systems.

#### 4.4. Adhesion agents

For dehumidification components such as DCHEs, adhesion agents/binders also play an important role in the heat transfer and moisture adsorption as they were added to desiccants to ensure the good adhesion on the substrate surface [95–97]. Considerations for the binder should include favorable adhesion properties, a positive effect on desiccant adsorption, satisfactory thermal conductivity, chemical inertness, and high durability [95].

The influences of binders on desiccant properties are summarized in Table 6. With the aim of investigating the effects of different filling densities and binder types on the porosity and thermal conductivity of desiccants, Younes et al. [98] directly synthesized composite desiccants with silica gel by using four types of binders, namely, hydroxyethyl cellulose, polyvinyl alcohol, polyvinyl pyrrolidone and gelatin respectively. By characterizing these composites and determining their thermal conductivity, it revealed that the filling density of composites had no negative effect on the porosity of silica gel and their thermal conductivity was rather enhanced compared to silica gel.

Besides, after selecting the suitable binder, a coating method needs to be chosen. The coating methods include the in-situ synthesis method, spraying method and impregnation coating method [91,95,102]. The in-situ synthesis method involves the synthesis of crystals on the matrix metal by selecting appropriate reactants. The spraying method disperses desiccants into uniform and fine droplets on the surface through special equipment such as spray guns or atomizers. The impregnation coating method forms the desiccant coating of a certain thickness on the metal surface by immersing it in the prepared solution.

#### 4.5. Comparative study

For a clearer comparison, the various composite desiccants mentioned are summarized, including the equilibrium adsorption quantity and desorption ability, adsorption-desorption kinetics and thermal COP.

##### 4.5.1. Equilibrium adsorption quantity and desorption ability

The primary objective of desiccants is to mitigate latent heat within cyclic operating conditions.

There is a large volume of published studies focusing on the equilibrium adsorption quantity and desorption ability of desiccants. To identify superior desiccants, Zheng et al. [38] conducted a comprehensive review of desiccants in 2014, as depicted in Fig. 20a. With the rapid development of materials science, the equilibrium adsorption quantity and desorption ability of desiccant materials have improved a lot. Here, desiccants prepared after 2015 are summarized in Fig. 20b.

Apparently, in Fig. 20a, there is a blank in Region I (equilibrium

**Table 6**  
The influences of binder on desiccant properties.

Binders	Desiccants	Properties	Ref
Sepiolite	Silica gel	Poor adhesive characteristics	[95]
Bentonite	Silica gel	Poor adhesive characteristics	[95]
Epoxy	Silica gel	Low BET surface area	[95]
Gelatin	Silica gel	Good adhesive characteristics	[95]
Polysiloxane	Aluminum fumarate	Improvement of heat transfer and excellent durability	[99]
Polyvinyl alcohol	AIPO-18	Low effect on hygroscopicity and an increase in adsorption heat.	[100]
Polyvinyl pyrrolidone	Silica gel	Improvement of heat transfer and low impact on water adsorption capacity of desiccant	[98]
silane	SAPO-34	Increased mechanical stability and without effect on the porosity of desiccants	[101]

adsorption quantity more than  $0.5 \text{ g g}^{-1}$  and desorption temperature less than  $60^\circ\text{C}$ ), that is, desiccants before 2015 fail to possess both high adsorption quantity and good desorption ability under low regeneration temperature such as at  $40\text{--}60^\circ\text{C}$ . For example, MIL-101(Cr) is able to achieve a fair adsorption quantity as high as  $1.7 \text{ g g}^{-1}$  but needs to be driven at  $70^\circ\text{C}$ . On the contrary, clay-based composites can be desorbed at  $40\text{--}60^\circ\text{C}$ , while their adsorption quantities are low ( $0.1\text{--}0.5 \text{ g g}^{-1}$ ). Currently, desiccants with excellent properties (in Regin I) gradually emerge. In particular, the utilization of a thermo-responsive polymer PNIPAM helps to obtain composite desiccants with excellent characteristics, namely, both high moisture adsorption capacity and good desorption ability. For instance, the adsorption capacity of SG/PNIPAM/LiCl can reach  $1.70 \text{ g g}^{-1}$  at  $20^\circ\text{C}$ &70% RH, and 56% of adsorbed moisture can be released within 60 min at  $40^\circ\text{C}$  [80].

Besides, salt-embedded composites (either porous matrix-based or polymer-based) usually have enhanced adsorption performance, but require to be driven under higher desorption temperatures ( $>80^\circ\text{C}$ ). On the other hand, salt-free composites such as porous matrix-polymer and polymer-polymer are able to avoid the corrosion problem and regenerate at lower desorption temperatures ( $40\text{--}80^\circ\text{C}$ ). However, the adsorption capacity of current salt-free composites is unsatisfactory.

##### 4.5.2. Adsorption-desorption kinetics

Undoubtedly, significant progress has been made in the equilibrium adsorption quantity and desorption ability of desiccant materials. In addition, for adsorption-based dehumidification systems, the cycle time for a single dehumidification or regeneration process is typically short, ranging from 300 s to 1200 s [11]. Therefore, the adsorption/desorption kinetics of desiccants also need to be taken into consideration. The dynamic adsorption and desorption curves of composites mentioned in Section 4 using LDF model are collected and depicted in Fig. 21a and (c), respectively. The test conditions for adsorption/desorption kinetics and  $k_{ad}/k_{de}$  in Fig. 21a and (c) are collected in Table 7.

From Fig. 21a, it can be seen that the dynamic adsorption capacity of salt-embedded composites is superior to that of salt-free composites. For a comprehensive presentation, the water adsorption capacity of these desiccants in the initial 50 min is presented in Fig. 21b. Under the same operating condition, desiccants impregnated with salt and polymer have a better dynamic adsorption capacity than only salt-embedded composites. For example, the water adsorption capacity of SG/PNIPAM/LiCl is  $0.89 \text{ g g}^{-1}$ , which is 3.3 times that of SG/LiCl. Among them, the aluminum fumarate/LiCl composite exhibits the most excellent performance of  $1.59 \text{ g g}^{-1}$ . Besides, the water adsorption capacity of graphene/LiCl composite with good thermal conductivity is  $0.34 \text{ g g}^{-1}$ , which is better than that of porous matrix-polymer composites and salt-embedded silica gel composites, but worse than that of polymer-salt composites. From Tables 7 and it can be seen that the graphene/LiCl composite also exhibits a large value of  $k_{ad}$ , representing faster adsorption kinetics.

Based on Fig. 21c, it can be observed that porous matrix-polymer composite desiccants present better desorption capacity compared to salt-embedded composite desiccants, exhibiting lower moisture content. For example, under the same desorption condition of  $40^\circ\text{C}$ &10% RH, the amount of water remaining in SG/PNIPAM at 150 min is  $0.03 \text{ g g}^{-1}$ , which is  $0.56 \text{ g g}^{-1}$  lower than that of SG/PNIPAM/LiCl.

For further comparison, Fig. 21d shows the water release of these desiccants in the initial 40 min and the next 40 min. It can be seen that released water amounts of all polymer-salt composites are higher than that of salt-free composites, particularly the aluminum fumarate/LiCl composite, which released the most in the first 40 min. The released water of SG/PNIPAM/LiCl, aluminum fumarate/LiCl, PAAS/LiCl, PAAS/KCOOH, PVA/LiCl, SG/LiCl and ENG-TSA/LiCl composite are  $0.69$ ,  $1.38$ ,  $1.23$ ,  $1.01$ ,  $1.24$ ,  $0.17$  and  $0.13 \text{ g g}^{-1}$  in the initial 40 min, corresponding to 51%, 86%, 59%, 89%, 70%, 28% and 29% of original water uptakes, respectively. The residual water amounts in MCM-41@EMIM Ac, AC/PAAS and SG/PNIPAM composite at 40 min

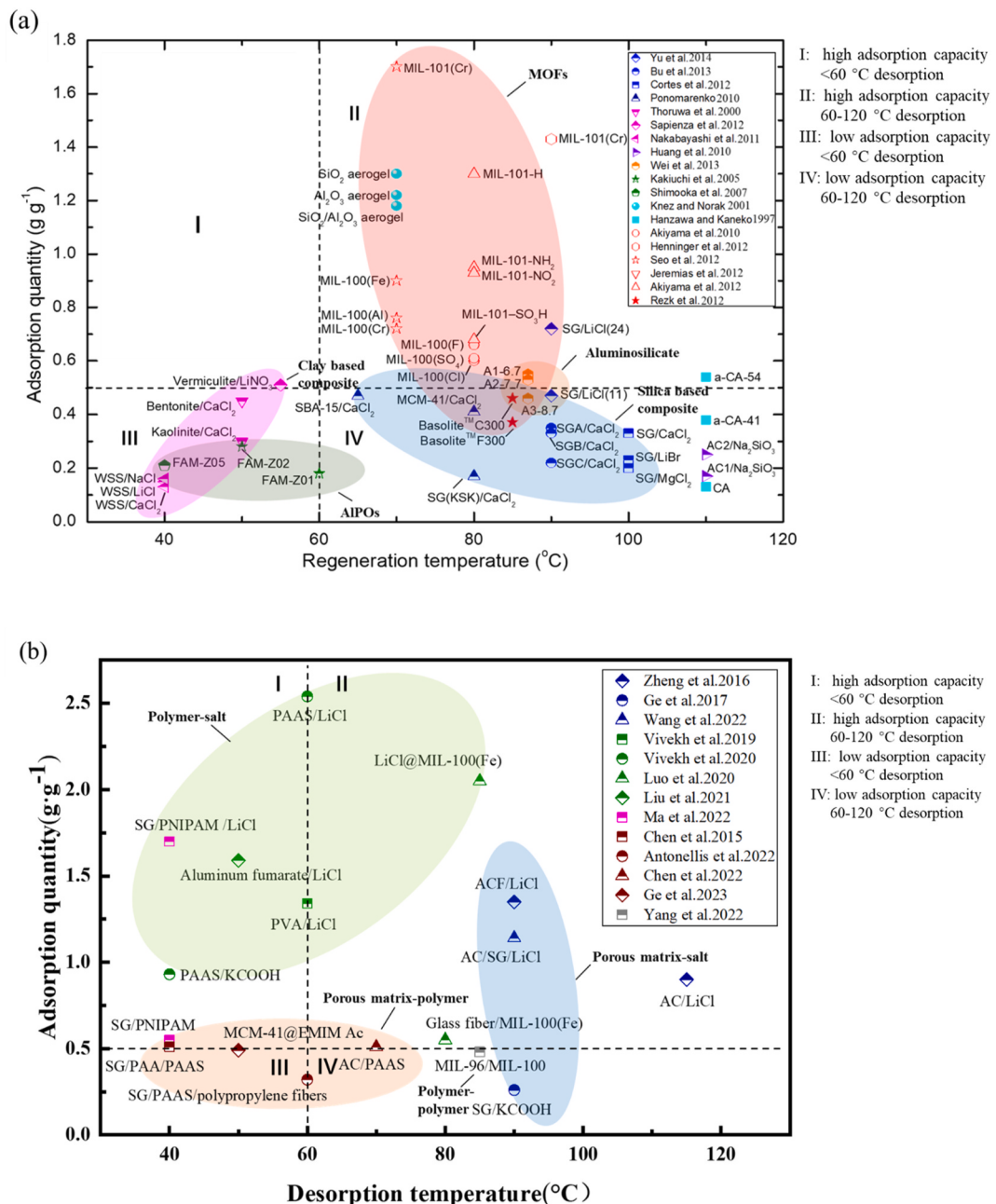


**Fig. 20.** Equilibrium adsorption quantity and desorption ability of reviewed desiccant materials: (a) before 2015 reproduced from Ref. [38] (Detailed data are shown in Tables 2, 3 and 5 of this Ref.) and (b) after 2015 from Refs. [46,61,62,66,68,73–75,78,80,83,84,86,88,89,91]. Detailed data of certain desiccants in Fig. 20(b) are mentioned in Tables 2–5.

are 0.06, 0.04 and 0.01 g g<sup>-1</sup>, occupied 13 %, 7 % and 2 % of the initial water uptakes, respectively. Because of the intrinsically low hygroscopic capacity of salt-free composite, complete desorption is basically achieved in the first 40 min (> 87 %).

Besides, the value of  $k_{de}$  is always higher than  $k_{ad}$ , and it is normally an order of magnitude larger than  $k_{ad}$ . It is worth noting that the adsorption and desorption periods should be reasonably arranged in a cycle time, with the desorption time being shorter than the adsorption time.

#### 4.5.3. Thermal COP of DCHE-based systems

For practical application, desiccants with desired properties need to be coated to the heat exchanger. Thermal COP ( $COP_{th}$ ) is an important indicator for evaluating DCHE-based systems. Higher regeneration

temperatures are beneficial for removing more water from the desiccant, but detrimental to COP<sub>th</sub> [104–106]. Although the internal fluids of DCHE-based systems are divided into water and HFCs, opting for water as a natural and environmentally friendly working fluid aligns well with the current carbon reduction policies.

The cooling efficiency of the system is characterized by COP<sub>th</sub>, defined as the ratio of the average cooling capacity on the air-side during the dehumidification process to the average heat consumed on the water-side during the regeneration process. Operating conditions of the most common silica gel and different composite desiccant coated heat exchangers (DCHEs) including inlet air temperature and relative humidity, cooling water temperature, heating water temperature and inlet air velocity are collected and listed in Table 8. The comparison with the COP<sub>th</sub> of DCHEs is presented in Fig. 22.

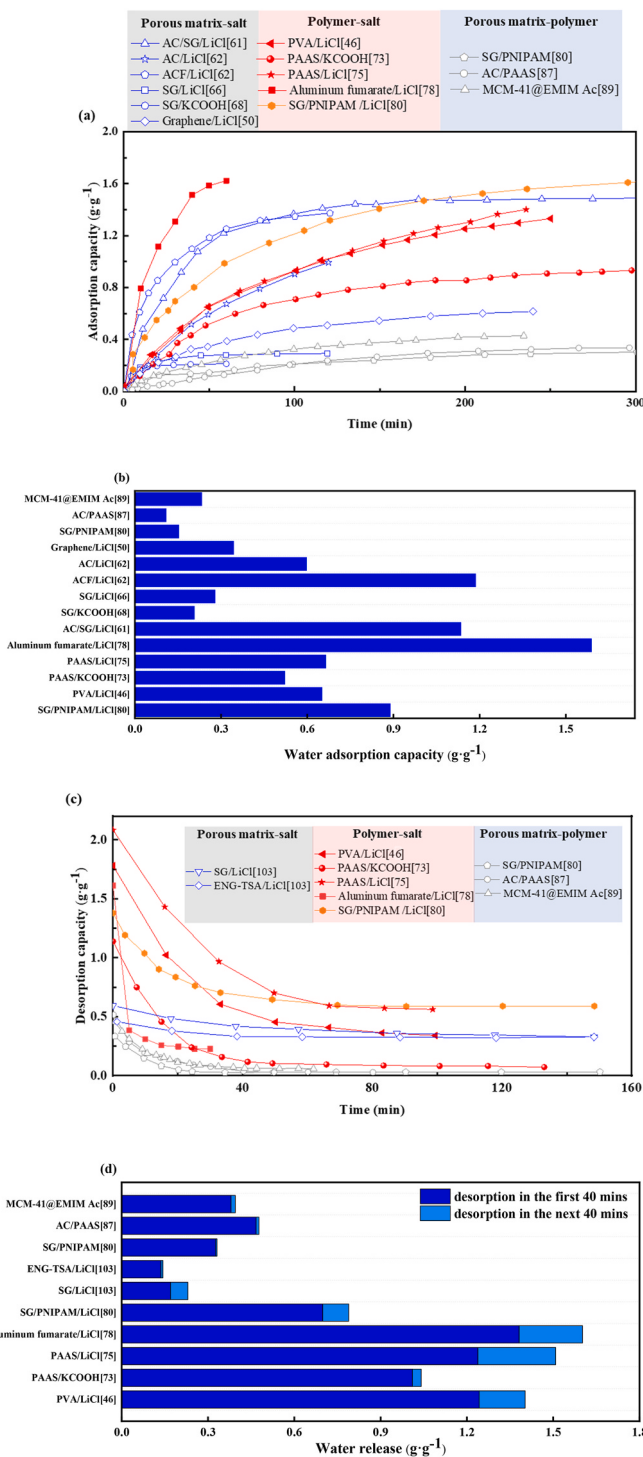


**Fig. 21.** Comparison of dynamic adsorption-desorption kinetics of different desiccants: adsorption kinetics curves (a), water adsorption capacity in the initial 50 min (b), desorption kinetics curves (c) and water release of desiccants in the initial 40 min and the next 40 min (d).

In general, the COP<sub>th</sub> of DCHEs declines with increasing regeneration temperatures. Ge et al. [105] prepared a silica gel-LiCl coated heat exchanger with the COP<sub>th</sub> improvement of 9%–12 % over the single silica gel coated heat exchanger at regeneration temperatures between 40 °C and 60 °C. The research by Vivekh et al. [46,73,107] demonstrated a 2–3 times enhancement in COP<sub>th</sub> when the heating water temperatures declined from 80 °C to 40 °C. The AC-PAAS coated heat exchanger produced by Zheng et al. [108] had a superior COP<sub>th</sub> due to

its ability to regenerate at low temperatures (40°C–50 °C). The reduction in COP<sub>th</sub> is caused by a proportion of the cooling capacity being used to cool down the higher temperature of the heat exchanger and more heating capacity being consumed for regeneration. Thus, for the practical application of DCHE-based systems, the desiccant should have both adsorption capacity and the ability to regenerate at low temperatures to further improve the COP<sub>th</sub> of systems.

## 5. Conclusions and perspectives

The adsorption-based dehumidification system offers a valuable alternative to conventional vapor compression systems for condensation dehumidification due to its capability to handle both sensible and latent heat, and the system has been investigated widely. The primary objective of this paper is to provide a comprehensive overview of recent developments in composite desiccants, directing at its application in adsorption-based dehumidification for energy efficient utilization.

Adding high thermal conductivity materials such as nano silver powder, expanded graphite, graphite sulfide and carbon nanotube can enhance heat transfer performance of adsorption-based dehumidification systems. Besides, good heat transfer and moisture adsorption properties can be achieved by reasonable structural design. For example, the performance of microchannel heat exchangers has been assessed by some researchers with progressive results compared to fin-and-tube heat exchangers in DCHE based systems.

The improvement of moisture adsorption can be strengthened by incorporating hygroscopic salts or by adding polymers compared to single desiccant material. Weak acid salts added to the porous matrix have the equilibrium adsorption capacity below 0.4 g·g<sup>-1</sup>. The equilibrium adsorption capacity of most composite desiccants can reach more than 1 g·g<sup>-1</sup> with the addition of strong hygroscopic salt. Besides, composites impregnated with polymers, as opposed to salt-embedded composites, generally exhibit the equilibrium adsorption capacity of less than 1 g·g<sup>-1</sup>.

MOF is gradually being developed as a promising material for composite desiccants. The adsorption capacity of MOF-salt composite desiccant is superior to that of porous matrix-salt composite desiccant under similar operating conditions. Most of the current research on MOF-based composite desiccant focuses on the properties of the material itself. However, there are few studies on the application of MOF-based composite desiccant to DCHE-based systems. The current desiccants practically applied to DCHE-based systems mainly concentrate on single porous matrix desiccant and porous matrix-salt composite desiccant.

Based on Fig. 20b, significant advancements have been achieved in the development of desiccant materials. Depending on the specific application scenario, appropriate desiccant materials can be chosen accordingly. For instance, for the utilization of life wastewater and condensation waste heat in the temperature range of 35–50 °C, thermo-responsive composite adsorbents are a suitable choice. For solar collectors operating at higher temperatures (70–90 °C), salt-embedded adsorbents can be a favorable option. In regions with non-humid climates like American Air-Conditioning and Refrigeration Institute (ARI) summer, salt-free composites can be used effectively. Considering factors such as desorption temperature, adsorption capacity and requirements of application, a comprehensive evaluation can be performed to determine the most suitable desiccant material.

Based on the comprehensive overview, promising approaches for future study to further enhance the energy efficiency of adsorption-based dehumidification technologies were summarized as follows.

- (1) Apart from adding high thermal conductivity materials to enhance the heat transfer of adsorption-based dehumidification, current research on the structure design of dehumidification component is relatively limited. For example, the majority of heat

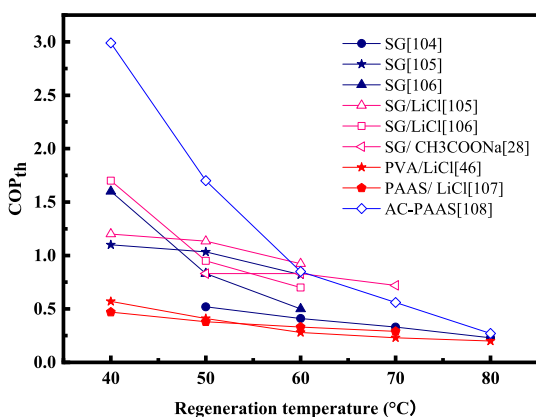
**Table 7**The operating conditions and  $k_{ad}/k_{de}$  of composite desiccants.

Desiccant	Adsorption temperature (°C)	Adsorption relative humidity (%RH)	$k_{ad}$	Desorption temperature (°C)	Desorption relative humidity (%RH)	$k_{de}$	Ref
Graphene/LiCl	20	70	$3.38 \times 10^{-4}$	–	–	–	[50]
SG/LiCl (40 wt %)	20	70	–	–	–	–	[66]
SG/KCOOH (75 wt %)	25	70	–	–	–	–	[68]
AC/SG/LiCl (40 wt %)	30	60	$2.26 \times 10^{-4}$	–	–	–	[61]
AC/LiCl (45 wt %)	20	70	$3.1 \times 10^{-4}$	–	–	–	[62]
ACF/LiCl (49 wt %)	20	70	$6.7 \times 10^{-4}$	–	–	–	[62]
PVA/LiCl (50 wt %)	30	80	$1.09 \times 10^{-4}$	60	0	$5.93 \times 10^{-4}$	[46]
PAAS/KCOOH (50 wt %)	20	80	$1.6 \times 10^{-4}$	40	5	$1.18 \times 10^{-3}$	[73]
PAAS/LiCl (50 wt %)	30	80	$6.1 \times 10^{-5}$	60	0	$7.29 \times 10^{-4}$	[75]
Aluminum fumarate/LiCl	22	70	–	70	0	–	[78]
SG/PNIPAM/LiCl (30 wt %)	20	70	$3.1 \times 10^{-4}$	40	10	$5.01 \times 10^{-3}$	[80]
SG/PNIPAM	20	70	$3.0 \times 10^{-4}$	40	10	$6.67 \times 10^{-3}$	[80]
AC/PAAS (50 wt %)	20	70	$1.6 \times 10^{-4}$	70	20	$1.5 \times 10^{-3}$	[86]
MCM-41@EMIM Ac	20	70	–	70	–	–	[89]
SG/LiCl (30 wt %)	25	70	–	77	20	–	[103]
ENG-TSA/LiCl	25	70	–	77	20	–	[103]

**Table 8**

The operating conditions and thermal COP of DCHEs.

Desiccant	Inlet air temp. (°C)	Inlet air humidity ratio ( $\text{g}\cdot\text{kg}^{-1}$ )	Cooling water temp. (°C)	Inlet air velocity ( $\text{m}\cdot\text{s}^{-1}$ )	Heating water temp. (°C)	$\text{COP}_{th}$	Ref
SG	30	21.57	30	0.39	50–80	0.23–0.52	[104]
SG	30	16.04	20	1.4	40–60	0.82–1.1	[105]
SG	30	16.04	15	1.54	40–60	0.5–1.6	[106]
SG/LiCl	30	16.04	15	1.54	40–60	0.7–1.7	[106]
SG/LiCl	30	16.04	20	1.4	40–60	0.91–1.18	[105]
SG/ CH <sub>3</sub> COONa	30	18.8	20	2.2	40–60	0.72–0.83	[28]
PVA/LiCl	30	21.5	30	0.39	40–80	0.2–0.57	[46]
PAAS/KCOOH	30	21.5	30	0.39	40	0.48	[73]
PAAS/LiCl	30	21.5	25	0.25	40–70	0.29–0.47	[107]
AC/PAAS	30	16.04	15	1.5	40–80	0.27–2.99	[108]

Fig. 22. Comparison with the  $\text{COP}_{th}$  of DCHEs in recent publications.

exchanger in DCHEs used is fin and tube ones. It is necessary to broaden the scope and explore other types of heat exchangers.

(2) The water vapor adsorption capacity of a single conventional desiccant can be strengthened by incorporating the strong

hygroscopic salt. However, the disadvantages such as corrosion and deliquescence can be resolved by controlling the concentration of salt or by adding organic weak acid salts or by selecting less corrosive polymers. Therefore, in the selection of desiccants, careful consideration of the advantages and disadvantages is necessary.

- (3) Most single desiccants such as porous physical adsorbents, chemical salts and polymer electrolytes have been commercialized, but MOF, a promising porous and hygroscopic material, has only been developed in small quantities in the laboratory without being produced on a large scale due to its high price. However, the concept of “MOF on MOF”, an in-situ synthesis on substrates without binder, offers a possible approach to this issue, making the mass production of MOFs possible. Besides, composite desiccants with excellent properties that are stuck in the laboratory stage are expected to be commercialized.
- (4) Despite the advantageous combination of high adsorption performance and low-temperature regeneration characteristics exhibited by thermo-responsive composites, their fabrication process remains complex and costly. Therefore, further research needs to pay attention to the optimization of synthesis procedures so as to achieve mass production.

- (5) Since the cycle time of adsorption-based dehumidification systems is typically short, desiccants do not necessarily reach their equilibrium adsorption capacity. Besides, according to the adsorption-desorption kinetic curves, the values of  $k_{de}$  tend to be an order of magnitude higher than those of  $k_{ad}$ . Thus, in future studies, it is not necessary to pursue high adsorption capacity excessively and each cycle has an optimal value proportional to the adsorption/desorption kinetics.
- (6) Under the regeneration process, the released moisture leads to a rapid rise in the humidity ratio of the outlet air. A condensing unit can be attached to the adsorption-based dehumidification system during desorption stage for water harvesting [109,110].

Experimental setups on adsorption-based dehumidification systems have been extensively constructed and studied with certain achievements. However, challenges remain exist in replacing the widely adopted traditional vapor compression dehumidification systems with this technology. Crucially, the research on adsorption-based dehumidification should not only concentrate on the enhancement of sorption capacities of desiccants but also on the stabilities and mass production to ensure an alternative to vapor compression dehumidification systems.

#### CRediT authorship contribution statement

**Yu Zhang:** Writing – original draft, Investigation, Formal analysis, Data curation. **Weining Wang:** Writing – review & editing. **Xu Zheng:** Funding acquisition, Conceptualization. **Jinliang Cai:** Data curation.

#### Declaration of competing interest

The authors declare that they have no known competing financial interests or personal relationships that could have appeared to influence the work reported in this paper.

#### Data availability

Data will be made available on request.

#### Acknowledgement

The work was supported by the Natural Science Foundation of Zhejiang Province, China (LY22E060004) and the National Natural Science Foundation of China (51806195).

#### References

- [1] Randazzo T, Cian ED, Mistry MN. Air conditioning and electricity expenditure: the role of climate in temperate countries. *Econ Model* 2020;90:273–87.
- [2] Wang Y, Zhang SH, Chow D, et al. Evaluation and optimization of district energy network performance: present and future. *Renew Sustain Energy Rev* 2021;139:110577.
- [3] Shamim JA, Hsu WL, Paul S, et al. A review of solid desiccant dehumidifiers: current status and near-term development goals in the context of net zero energy buildings. *Renew Sustain Energy Rev* 2021;137:110456.
- [4] Tu YD, Wang RZ, Ge TS, et al. Comfortable, high-efficiency heat pump with desiccant-coated, water-sorbing heat exchangers. *Sci Rep* 2017;7:40437.
- [5] Zhao LH, Wang RZ, Ge TS. Desiccant coated heat exchanger and its applications. *Int J Refrig* 2021;130:217–32.
- [6] Abou-Ziyan H, El-Raheem DA, Mahmoud O, et al. Performance characteristics of thin-multilayer activated alumina bed. *Appl Energy* 2017;190:29–42.
- [7] Tu R, Liu XH, Jiang Y. Performance analysis of a new kind of heat pump-driven outdoor air processor using solid desiccant. *Renew Energy* 2013;57:101–10.
- [8] Behere B, Chakrabarti S, Wankhede U, et al. Review on nanoporous inorganic desiccant materials in the context of application in rotary dehumidifiers. *Mater Today Proc* 2022;57:2174–9.
- [9] Zheng X, Wang RZ, Ma WX. Dehumidification assessment for desiccant coated heat exchanger systems in different buildings and climates: fast choice of desiccants. *Energy Build* 2020;221:110083.
- [10] Sun XY, Hua LJ, Dai YJ, et al. Field synergy analysis on heat and moisture transfer processes of desiccant coated heat exchanger. *Int J Therm Sci* 2021;164:106889.
- [11] Zhao Y, Ge TS, Dai YJ, et al. Experimental investigation on a desiccant dehumidification unit using fin-tube heat exchanger with silica gel coating. *Appl Therm Eng* 2014;63:52–8.
- [12] Vivekh P, Kumja M, Bui DT, et al. Recent developments in solid desiccant coated heat exchangers - a review. *Appl Energy* 2018;229:778–803.
- [13] Liu HY, Sundarraj S, Kumar GV, et al. Review on polymer materials for solid desiccant cooling system. *Macromol Mater Eng* 2023;1438–7492.
- [14] Feng YH, Dai YJ, Wang RZ, et al. Insights into desiccant-based internally-cooled dehumidification using porous sorbents: from a modeling viewpoint. *Appl Energy* 2022;311:118732.
- [15] Venegas T, Qi M, Nawaz K, et al. Critical review and future prospects for desiccant coated heat exchangers: materials, design, and manufacturing. *Renew Sustain Energy Rev* 2021;151:111531.
- [16] Chai SW, Chen ER, Xie MX, et al. Experimental study of dehumidification performance and solar thermal energy enhancement properties on a dehumidification system using desiccant coated heat exchanger. *Energy* 2022; 259:124983.
- [17] Sun XY, Dai YJ, Ge TS, et al. Investigation on humidification effect of desiccant coated heat exchanger for improving indoor humidity environment in winter. *Energy Build* 2018;165:1–14.
- [18] Hua LJ, Ge TS, Wang RZ. Extremely high efficient heat pump with desiccant coated evaporator and condenser. *Energy* 2019;170:569–79.
- [19] Hua LJ, Jiang Y, Ge TS, et al. Experimental investigation on a novel heat pump system based on desiccant coated heat exchangers. *Energy* 2018;142:96–107.
- [20] Zheng X, Wang RZ, Tu YD. Investigation on energy consumption of desiccant coated heat exchanger based heat pump: limitation of adsorption heat of desiccant. *Energy Convers Manag* 2019;188:473–9.
- [21] Bongs C, Morgenstern A, Lukito Y, et al. Advanced performance of an open desiccant cycle with internal evaporative cooling. *Sol Energy* 2014;104:103–14.
- [22] Sunil N, Anuradha P, Sanjay K. Experimental study and analysis of solar based winter air conditioning system using desiccant coated heat exchanger. *Materials Today: Proceedings* 2021;46:9938–43.
- [23] Sun XY, Chen JL, Zhao Y, et al. Experimental investigation on a dehumidification unit with heat recovery using desiccant coated heat exchanger in waste to energy system. *Appl Therm Eng* 2021;185:116342.
- [24] Xu F, Bian ZF, Ge TS, et al. Analysis on solar energy powered cooling system based on desiccant coated heat exchanger using metal-organic framework. *Energy* 2019;177:211–21.
- [25] Prabakaran V, Bui DT, Islam MR, et al. Studying the energy efficiency feasibility of composite superabsorbent coated heat exchangers in open-cycle heat transformation applications. *Energy Convers Manag* 2022;266:115867.
- [26] Kumar A, Yadav A. Experimental investigation of solar-powered desiccant cooling system by using composite desiccant "CaCl<sub>2</sub>/jute". *Environ Dev Sustain* 2017;19(4):1279–92.
- [27] Dasar SR, Boche AM, Yadav AK, et al. Sorption-desorption characteristics of dried cow dung with PVP and clay as composite desiccants: experimental and energetic analysis. *Renew Energy* 2023;202:394–404.
- [28] Valarezo AS, Sun XY, Ge TS, et al. Experimental investigation on performance of a novel composite desiccant coated heat exchanger in summer and winter seasons. *Energy* 2019;166:506–18.
- [29] Park B, Lee S. Investigation on heat and mass transfer characteristics for a zeolite-coated heat exchanger using comparatively low-temperature energy: heating humidification mode and cooling dehumidification mode. *Indoor Built Environ* 2021;309(1486):1502.
- [30] La D, Dai YJ, Li Y, et al. Technical development of rotary desiccant dehumidification and air conditioning: a review. *Renewable Sustainable Energy Rev* 2010;14(1):130–47.
- [31] Wang C, Ji X, Yang BF, et al. Study on heat transfer and dehumidification performance of desiccant coated microchannel heat exchanger. *Appl Therm Eng* 2021;192:116913.
- [32] Wang JY, Wang RZ, Wang LW, et al. A high efficient semi-open system for fresh water production from atmosphere. *Energy* 2017;138:542–51.
- [33] Hsu WL, Paul S, Shamim JA, et al. Design and performance evaluation of a multilayer fixed-bed binder-free desiccant dehumidifier for hybrid air-conditioning systems: Part II-Theoretical analysis. *Int J Heat Mass Tran* 2018;116:1370–8.
- [34] Hua LJ, Sun XY, Jiang Y, et al. Graphic general solutions for desiccant coated heat exchangers based on dimensional analysis. *Int J Heat Mass Tran* 2020;2020:119654.
- [35] Mauer LJ, Taylor LS. Water-solids interactions: deliquescence. *Annu Rev Food Sci Technol* 2010;1:41–63.
- [36] Wang Y, Liu J, Zhang YR, et al. Advances in polymer desiccant. *Mod Chem Ind* 2019;39(S1):99–103 (in Chinese).
- [37] Ng EP, Mintova S. Nanoporous materials with enhanced hydrophilicity and high water sorption capacity. *Microporous Mesoporous Mater* 2008;114:1–26.
- [38] Zheng X, Wang RZ, Ge TS. Recent progress on desiccant materials for solid desiccant cooling systems. *Energy* 2014;74:280–94.
- [39] Krishnan EN, Ramin H, Gurubalan A, Simonson CJ. Experimental methods to determine the performance of desiccant coated fixed bed e d regenerators (FBRs). *Int J Heat Mass Tran* 2022;182:121909.
- [40] Ramin H, Krishnan EN, Gurubalan A, et al. A transient numerical model for sensible fixed-bed regenerator in HVAC applications. *Int J Heat Mass Tran* 2021; 177:1212550.
- [41] Li BJ, Hua LJ, Tu YD, et al. A full-solid-state humidity pump for localized humidity control. *Joule* 2019;3(6):1427–36.

- [42] Sultan M, El-Sharkawy II, Miyazaki T, et al. Water vapor sorption kinetics of polymer based sorbents: theory and experiments. *Appl Therm Eng* 2016;106:192–202.
- [43] Yao Y, Dai L, Jiang FJ, et al. Kinetic modeling of novel solid desiccant based on PVA-LiCl electrospun nanofibrous membrane. *Polym Test* 2018;64:183–93.
- [44] Büker MS, Parlaklı H, Alwetaishi M, et al. Experimental investigation on the dehumidification performance of a parabolic trough solar air collector assisted rotary desiccant system. *Case Stud Therm Eng* 2022;34:102077.
- [45] Gouanne F, Marais S, Bessadok A, et al. Kinetics of water sorption in flax and PET fibers. *Eur Polym J* 2007;43:586–98.
- [46] Vivekh P, Bui DT, Wong Y, et al. Performance evaluation of PVA-LiCl coated heat exchangers for next generation of energy-efficient dehumidification. *Appl Energy* 2019;237:733–50.
- [47] Wang JY, Wang RZ, Tu YD, et al. Universal scalable sorption-based atmosphere water harvesting. *Energy* 2018;165:387–95.
- [48] Zheng X, Lin Z, Xu BF. Thermal conductivity and sorption performance of nano-silver powder/FAPO-34 composite fin. *Appl Therm Eng* 2019;160:114055.
- [49] Wu S, Li QY, Ikuta T, et al. Thermal conductivity measurement of an individual millimeter-long expanded graphite ribbon using a variable-length T-type method. *Int J Heat Mass Tran* 2021;171:121115.
- [50] Zheng X, Wang RZ. Microstructure and sorption performance of consolidated composites impregnated with LiCl. *Int J Refrig* 2019;98:452–8.
- [51] Zheng X, Wang LW, Wang RZ, et al. Thermal conductivity, pore structure and adsorption performance of compact composite silica gel. *Int J Heat Mass Tran* 2014;68:435–43.
- [52] Hua WS, Xie WH, Zhang XL, et al. Synthesis and characterization of silica gel composite with thermal conductivity enhancers and polymer binders for adsorption desalination and cooling system. *Int J Refrig* 2022;139:93–103.
- [53] Xie WH, Hua WS, Zhang XL, et al. Preparation and characteristics analysis of the new-type silica gel/CaCl<sub>2</sub> adsorbents with nanoparticles for adsorption desalination and cooling system. *J Sol Gel Sci Technol* 2023;105(2):525–36.
- [54] Starkova O, Chandrasekaran S, Schnoor T, et al. Anomalous water diffusion in epoxy/carbon nanoparticle composites. *Polym Degrad Stabil* 2019;164:127–35.
- [55] Fu HX, Yang QR, Zhang LZ. Effects of material properties on heat and mass transfer in honeycomb-type adsorbent wheels for total heat recovery. *Appl Therm Eng* 2017;118:345–56.
- [56] Park MH, Chung JY, Hong SH, et al. Performance characteristics of desiccant rotor using metal organic framework material. *Appl Therm Eng* 2023;223:120066.
- [57] Mitra S, Aswin N, Dutta P. Scaling analysis and numerical studies on water vapour adsorption in a columnar porous silica gel bed. *Int J Heat Mass Tran* 2016;95:853–64.
- [58] Sun XY, Dai YJ, Ge TS, et al. Heat and mass transfer comparisons of desiccant coated microchannel and fin-and-tube heat exchangers. *Appl Therm Eng* 2019;150:1159–67.
- [59] Li A, Thu K, Bin Ismail A, et al. Performance of adsorbent-embedded heat exchangers using binder-coating method. *Int J Heat Mass Tran* 2016;92:149–57.
- [60] Lertboonkankit P, Chirattananon S. Experimental investigation on a desiccant air dehumidifier constructed from a water-to-air heat exchanger. *Energy Proc* 2017;138:628–34.
- [61] Wang C, Yang BF, Ji X, et al. Study on activated carbon/silica gel/lithium chloride composite desiccant for solid dehumidification. *Energy* 2022;251:123874.
- [62] Zheng X, Wang RZ, Ge TS. Experimental study and performance predication of carbon based composite desiccants for desiccant coated heat exchangers. *Int J Refrig* 2016;72:124–31.
- [63] Zheng X, Wang RZ, Ge TS, et al. Performance study of SAPO-34 and FAPO-34 desiccants for desiccant coated heat exchanger systems. *Energy* 2015;93(Part 1):88–94.
- [64] Sunhor S, Osaka Y, Tsujiguchi T, et al. Dehumidification behavior of an aluminophosphate zeolite coated crossflow heat exchanger driven with direct hot water heating and evaporative cooling. *Appl Therm Eng* 2022;210:118355.
- [65] Liu L, Kubota M, Li J, et al. Comparative study on the water uptake kinetics and dehumidification performance of silica gel and aluminophosphate zeolites coatings. *Energy* 2022;242:122957.
- [66] Zheng X, Ge TS, Jiang Y, et al. Experimental study on silica gel-LiCl composite desiccants for desiccant coated heat exchanger. *Int J Refrig* 2015;51:24–32.
- [67] Hu LM, Ge TS, Jiang Y, et al. Performance study on composite desiccant material coated fin-tube heat exchangers. *Int J Heat Mass Tran* 2015;90:109–20.
- [68] Ge TS, Zhang JY, Dai YJ, et al. Experimental study on performance of silica gel and potassium formate composite desiccant coated heat exchanger. *Energy* 2017;141:149–58.
- [69] Higashi T, Zhang L, Saikawa M, et al. Theoretical and experimental studies on isothermal adsorption and desorption characteristics of a desiccant-coated heat exchanger. *Int J Refrig* 2017;84:228–37.
- [70] Xu F, Zhang M, Cui YX, et al. A novel polymer composite coating with high thermal conductivity and unique anti-corrosion performance. *Chem Eng J* 2022;439:135660.
- [71] Jeremias F, Khutia A, Henninger SK, et al. MIL-100(Al, Fe) as water adsorbents for heat transformation purposes—a promising application. *J Mater Chem* 2012;22:10148–51.
- [72] Chang CC, Luo WJ, Lu CW, et al. Effects of process air conditions and switching cycle period on dehumidification performance of desiccant-coated heat exchangers. *Science and Technology for the Built Environment* 2017;23(1):81–90.
- [73] Vivekh P, Bui DT, Islam MR, et al. Experimental performance and energy efficiency investigation of composite superabsorbent polymer and potassium formate coated heat exchangers. *Appl Energy* 2020;275:115428.
- [74] Luo YS, Tan BQ, Liang XH, et al. Investigation on water vapor adsorption performance of LiCl@MIL-100(Fe) composite adsorbent for adsorption heat pumps. *Int J Energy Res* 2020;44(7):5895–904.
- [75] Vivekh P, Islam MR, Chua KJ. Experimental performance evaluation of a composite superabsorbent polymer coated heat exchanger based air dehumidification system. *Appl Energy* 2020;260:114256.
- [76] Tan BQ, Luo YS, Liang XH, et al. Composite salt in MIL-101(Cr) with high water uptake and fast adsorption kinetics for adsorption heat pumps. *Microporous Mesoporous Mater* 2019;286:141–8.
- [77] Elsayed E, Anderson P, Al-Dahad R, et al. MIL-101(Cr)/calcium chloride composites for enhanced adsorption cooling and water desalination. *J Solid State Chem* 2019;277:123–32.
- [78] Liu ZB, Cheng CJ, Han JD, et al. Dehumidification performance of aluminum fumarate metal organic framework and its composite. *Appl Therm Eng* 2021;199:117570.
- [79] Yang YF, Rana D, Lan CQ. Development of solid super desiccants based on a polymeric superabsorbent hydrogel composite. *RSC Adv* 2015;5(73):59583–90.
- [80] Ma QL, Zheng X. Preparation and characterization of thermo-responsive composite for adsorption-based dehumidification and water harvesting. *Chem Eng J* 2022;429:132498.
- [81] Zheng X, Chen K, Lin Z. Synthesis and characterization of Alginate–Silica gel composites for adsorption dehumidification. *Ind Eng Chem Res* 2020;59:5760–7.
- [82] Entezari A, Ejteian M, Wang RZ. Super atmospheric water harvesting hydrogel with alginate chains modified with binary salts. *ACS Mater Lett* 2020;2:471–7.
- [83] Chen CH, Hsu CY, Chen CC, et al. Silica gel polymer composite desiccants for air conditioning systems. *Energy Build* 2015;101:122–32.
- [84] Antonellis SD, Bramanti E, Calabrese L, et al. A novel desiccant compound for air humidification and dehumidification. *Appl Therm Eng* 2022;214:118857.
- [85] Calabrese L, Bonaccorsi L, Bruzzaniti P, et al. SAPO-34 based zeolite coatings for adsorption heat pumps. *Energy* 2019;187:115981.
- [86] Chen K, Zheng X, Wang SN. Investigation on activated carbon-sodium polyacrylate coated aluminum sheets for desiccant coated heat exchanger. *Energy* 2022;245:123206.
- [87] Liu L, Wu RJ, Li J, et al. Experimental and theoretical study on water vapor isothermal adsorption-desorption characteristics of desiccant coated adsorber. *Int J Heat Mass Tran* 2022;187:122529.
- [88] Luo YS, Tan BQ, Liang XH, et al. Dry gel conversion synthesis and performance of glass-fiber MIL-100(Fe) composite desiccant material for dehumidification. *Microporous Mesoporous Mater* 2020;297:110034.
- [89] Ge LR, Feng YH, Dai YJ, et al. Imidazolium-based ionic liquid confined into ordered mesoporous MCM-41 for efficient dehumidification. *Chem Eng J* 2023;452:139116.
- [90] Hermes S, Schroder F, Chelmowski R, et al. Selective nucleation and growth of metal-organic open framework thin films on patterned COOH/CF<sub>3</sub>-terminated self-assembled monolayers on Au(111). *J Am Chem Soc* 2005;127:13744–5.
- [91] Yang TY, Ge LR, Ge TS, et al. Binder-free growth of aluminum-based metal-organic frameworks on aluminum substrate for enhanced water adsorption capacity. *Adv Funct Mater* 2022;32:2105267.
- [92] Gu XP, Han GP, Yang QY, et al. Confinement–unconfinement transformation of ILs in IL MOF composite with multiple adsorption sites for efficient water capture and release. *Adv Mater Interfac* 2022;9:2102354.
- [93] Qin MH, Feugas O, Zu K. Novel metal-organic framework (MOF) based phase change material composite and its impact on building energy consumption. *Energy Build* 2022;273:112382.
- [94] Karmakar A, Mileo P, Bok I, et al. Thermo-responsive MOF/polymer composites for temperature mediated water capture and release. *Angew Chem Int Ed* 2020;59:11003–9.
- [95] Li A, Thu K, Bin Ismail A, et al. Performance of adsorbent-embedded heat exchangers using binder-coating method. *Int J Heat Mass Tran* 2016;92:149–57.
- [96] Ang L, Kyaw T, Karan MS, et al. Binder influence on the water adsorption uptake of silica gel. *Appl Mech Mater* 2016;819:176–80.
- [97] Shamim JA, Paul S, Hsu WL, et al. Theoretical analysis of transient heat and mass transfer during regeneration in multilayer fixed-bed binder-free desiccant dehumidifier: model validation and parametric study. *Int J Heat Mass Tran* 2019;134:1024–40.
- [98] Younes MM, El-sharkawy I, Kabeel AE, et al. Synthesis and characterization of silica gel composite with polymer binders for adsorption cooling applications. *Int J Refrig* 2019;98:161–70.
- [99] Kummer H, Jeremias F, Warlo A, et al. A functional full-scale heat exchanger coated with aluminum fumarate metal-organic framework for adsorption heat transformation. *Ind Eng Chem Res* 2017;56:8393–8.
- [100] Chang KS, Chen MT, Chung TW. Effects of the thickness and particle size of silica gel on the heat and mass transfer performance of a silica gel-coated bed for air-conditioning adsorption systems. *Appl Therm Eng* 2005;25:2330–40.
- [101] Calabrese L, Brancato V, Bonaccorsi L, et al. Development and characterization of silane-zeolite adsorbent coatings for adsorption heat pump applications. *Appl Therm Eng* 2017;116:364–71.
- [102] Fang YT, Zuo SQ, Liang XH, et al. Preparation and performance of desiccant coating with modified ion exchange resin on finned tube heat exchanger. *Appl Therm Eng* 2016;93(25):36–42.
- [103] Wang JY, Liu YJ, Wang RZ, et al. Experimental research of composite solid sorbents for fresh water production driven by solar energy. *Appl Therm Eng* 2017;121:941–50.

- [104] Oh SJ, Ng KC, Chun W, Chua KJE. Evaluation of a dehumidifier with adsorbent coated heat exchangers for tropical climate operations. *Energy* 2017;137(15): 441–8.
- [105] Ge TS, Cao W, Pan X, Dai YJ, Wang RZ. Experimental investigation on performance of desiccant coated heat exchanger and sensible heat exchanger operating in series. *Int J Refrig* 2017;83:88–98.
- [106] Jiang Y, Ge TS, Wang RZ, Hu LM. Experimental investigation and analysis of composite silica-gel coated fin-tube heat exchangers. *Int J Refrig* 2015;51: 169–79.
- [107] Vivekh P, Islam MR, Chua KJ. Experimental performance evaluation of a composite super absorbent polymer coated heat exchanger based air dehumidification system. *Appl Energy* 2020;260:114256.
- [108] Zheng X, Zhang Y, Wan TH, Chen K. Experimental study on the performance of a novel superabsorbent polymer and activated carbon composite coated heat exchangers. *Energy* 2023;281:128293.
- [109] Ejelian M, Wang RZ. Adsorption-based atmospheric water harvesting. *Joule* 2021; 5(7):1678–703.
- [110] Shafeian N, Ranjbar AA, Gorji TB. Progress in atmospheric water generation systems: a review. *Renew Sustain Energy Rev* 2022;161:112325.